

Two Phase Simulation of Ultrarelativistic Nuclear Collisions

D. E. Kahana², S. H. Kahana¹

¹*Physics Department, Brookhaven National Laboratory
Upton, NY 11973, USA*

²*Physics Department, State University of New York,
Stony Brook, NY 11791, USA*

(February 13, 2018)

A two phase cascade is presented for the treatment of ultra-high energy ion-ion collisions from $\sqrt{s} = 17 - 200$ GeV. First a high energy, fast cascade is performed, in which original baryons and freed hard partons, if any, collide. This stage ignores energy loss from soft (slow) processes. In this first version in fact, no hard processes, aside from Drell-Yan production, are included. The space-time history of the hard cascade is then used as input to reconstruct the soft energy-loss, which occurs over a longer time scale. Soft meson production is therefore treated as coherent over groups of interacting nucleons. Two body data, though, are used extensively to guide this reinitialisation of the cascade, which satisfies conservation laws for charge, strangeness and of course, energy-momentum. A second, low energy, cascade is finally carried out among the products of the hard cascade. The model selected to describe elementary hadron-hadron collisions in the soft cascade incorporates generic mesons and baryons, which are the agents for rescattering. We imagine a constituent quark model applies, with generic mesons consisting of an excited $q\bar{q}$ pair, and generic baryons constructed from three quarks. The chief result is a reconciliation of the important Drell-Yan measurements, indicating high-mass lepton pairs are produced *as if no energy is lost from the nucleons*, with the apparent success of a purely hadronic, soft cascade in describing nucleon stopping and meson production in heavy ion experiments at the CERN SPS.

25.75, 24.10.Lx, 25.70.Pq

I. INTRODUCTION

Many cascades [1–9] have been constructed to consider relativistic heavy ion collisions. Since the eventual aim of experiments designed to study such collisions is the creation of a regime in which the quark-gluon structure of hadronic matter becomes evident, it is ultimately necessary to include partonic degrees of freedom in such cascades. However, since at SPS and even at RHIC energies it is by no means clear that all initial or subsequent hadron-hadron collisions occur with sufficient transverse momentum to free all partons [10], any complete simulation must deal, at least in part, initially with collisions of the original nucleons, and finally with collisions of all the produced hadrons. We will regard the extent to which partons play a role in the initial stage as an open question. In the course of laying out potential algorithms for the hadronic sector of the cascade, there arises a very natural, time-scale driven division between hadronic and partonic sectors. We present in this work

the architecture of a new ultra-high energy cascade, including its hadronic cross-section inputs, and a detailed description of the algorithms.

To begin, we wish to discuss the global time scales which divide the cascade into sectors one could designate as ‘hard, perturbative QCD, or partonic’, and ‘soft, non-perturbative QCD, or hadronic’. This classification has been discussed often in the literature [10–16]. For our purposes here a general outline will suffice. Experimental results [17] on both energy loss and forward pion production in high energy proton-nucleus scattering were the key motivation for this reasoning. Energy-loss through meson production at low transverse momentum p_T is in general a ‘slow’ process. In contrast to this stand ‘fast’ or hard processes, of which Drell-Yan pair production (DY) [18–20], which we will consider in some detail, is a good example. Characteristic time scales for these processes can in the first approximation be inferred from the uncertainty principle. Small momentum transfer meson production takes a long time $\tau_f \sim p_T^{-1}$, while production of lepton pairs with high mass, in excess of say $M_{\mu\mu} \sim 4$ GeV takes much less time, $\tau_h \sim 1/M_{\mu\mu}$.

If one examines Drell-Yan data [19] in high energy pA collisions, Fig(1), the apparent A -dependence of the DY cross-section $\sigma_{DY} \sim A$ suggests that all production of high mass pairs takes place *at the highest energy*, that is, at the energy of the initial pp collision. The incoming proton simply counts every nucleons that it hits, and has an equal probability of producing a DY pair in each collision. This stands in direct opposition to one’s naïve expectation for a standard hadronic two body cascade, in which successive collisions of the leading baryon take place at lower and lower energies, predicting that σ_{DY} should rise more slowly than A . Pion numbers found in pA for the highest Feynman x in similar collisions [17] also show little increase above that expected from pp at the incoming energy. These results together imply the initiating proton has, in producing DY pairs, suffered no energy loss in its passage through the nucleus. Nevertheless, calculations with a purely hadronic cascade [9] describe very well the large energy loss represented in the inclusive pion spectrum observed in massive Pb+Pb collisions at SPS energies (see Fig 2). It is as if, even though the protons in their initial interactions inside a nucleus do not lose appreciable energy, they nevertheless remember full well what number and sort of collisions they have experienced. The question then is, can the initial energy retention characteristic of Drell-Yan and eventual energy loss into meson production be described in a unified dynamic fashion.

It should be noted that the reason for this break down in the pure two body cascade in ultra-high energy ion-ion collisions is that the soft time scale τ_f (for meson production) has become longer than the time scale τ_c for the projectile to pass through the target. Therefore soft energy loss cannot occur before all the hard collisions have taken place.

These apparently contradictory features can in fact be put together in a single particle or resonance-based multiscattering scheme, simply and in a rather robust fashion. Gottfried [11] has suggested a mechanism to describe leading particle behaviour in pA, which we discussed and implemented in an earlier effort [9] at building a simulation code, which tracks the time evolution of a highly Lorentz contracted and excited proton into its final state, including all the mesons expected to be produced in a free space nucleon-nucleon interaction. These mesons are inhibited from independently interacting with the target nucleus until they separate in space from the leading baryon by some minimum hadronic size. This mechanism ensures that in very high energy pA collisions the leading proton retains very nearly its incoming energy for most of its passage through the nucleus. A

similar criterion for ‘re-joining’ produced particles was incorporated by us into a hadronic cascade and this did quite well in the description of DY production in the FNAL 800 GeV/c pA data [19].

We have decided here, however, to proceed in what is in the end a simpler fashion, separating soft and hard processes by time scale, and thus permitting partonic and hadronic cascading to be put together very naturally and smoothly, and in a modular fashion. The method simply consists of running the cascade in two phases, the first a high energy / short time phase in which collision histories are recorded and fast processes are allowed to engage. This stage ends at time τ_c , when the projectile and target nuclei have completely passed through each other. Then, using the space-time history of the first phase, a reinitialisation of the cascade is performed and a second phase, consisting of a normal soft hadronic cascade is carried out, at greatly reduced energy and over longer times. Figure (3) shows the final positions of baryons after the first phase, and the almost light-like paths for the particles engaging in the initial cascade.

The reinitialization is most critical and is generated from the detailed space-time history acquired during the initial high energy cascading. The procedure followed is first to set up groups of nucleons which have mutually collided in the initial phase of the cascade. Energy loss can then be computed for *each* nucleon using its known trajectory and collision history, and the measured inelasticity of the nucleon-nucleon interaction. Nucleon-nucleon collision data, from the initial energy down, provide the information on multiplicity distributions, rapidity distributions, and the correlation of these distributions with energy loss, which is essential in determining the final baryon four-momenta and hence the energy and momentum to be deposited on mesons. The method employed is described in detail below but proceeds as closely as possible to reconstructing the two-body scatterings experienced by each nucleon traced. Thus fluctuations, inherent in NN scattering, in the energy loss and in multiplicity, are mirrored in the reinitialisation. Generic meson resonances are then added in, group by group, so that all applicable conservation laws are obeyed. The cascade is then re-initialised, and restarted at the time of the last high energy nucleon-nucleon collision that occurred in the high energy stage. Generic meson resonances are the principal rescatterers in the ensuing low-energy cascade together with the still present, much slowed, baryons.

Partonic casacading at sufficiently high momentum transfer could also have proceeded during the initial stage, taking place over the short time scale associated with a high momentum transfer. The energy-momentum taken out of nucleons by such hard partons would have to be subtracted from that available for the final production of soft mesons among the ‘nucleon’ groups, but it would eventually reappear in the meson sector as the hard partons completed their dynamics and re-hadronised. Indeed the time scale for hadronisation is comparable to the formation time τ_f for the soft mesons, so in a first approximation, the mesons produced by parton dynamics might simply be added to the reinitialisation before restarting the final soft phase.

One might refer to this two stage cascade as an effective separation into short and long distance behaviour, a separation created by a factorisation of the time scales, or equivalently by the momentum transfer involved in each process. As we mentioned previously, there is an extensive literature on this subject [11–16,21].

The two phase approach discussed here has a highly beneficial effect on what one might fear could be a serious shortcoming of relativistic cascades in general, that there might be a

strong frame dependence. Preliminary calculations at RHIC energy, $\sqrt{s} = 200$ GeV/A, for a central Au+Au collision, constituting in the present context a worst case scenario, show that the pion dN/dy differs by no more than 10-15% between two extreme cases: a cascade carried out in the global lab frame with $\gamma \sim 20,000$, and a cascade performed in the global center of mass frame with $\gamma \sim 100$ (see Figure 4). The results in the latter figure must be considered very preliminary for RHIC collisions and represent no more than a rough prediction for mesons, still less for protons. We intend here only to illustrate the worst possible extent of the frame dependence to be expected in our cascade at RHIC energies. This dependence is moderate as indicated. At SPS energy, the frame dependence is very small, any differences being negligible and within present statistical errors.

The reason for the minimal frame dependence is simple and systemic: the initial high energy cascade contains only particles travelling along nearly light-like paths (see Fig(3)), and the light cone is, of course, an invariant surface. Therefore, *the re-initialisation does not depend upon the global frame chosen for the cascade*. Any frame dependence enters only in the second phase, which involves greatly reduced collision energies and particle densities. The separation into two stages thus greatly ameliorates frame dependence.

The second phase involves generic resonances, strange and non-strange, with the quantum numbers of the Δ , the N^* , the Σ and the Λ in the baryon sector, and those of the ρ , and the K in the meson sector, with masses in the range $m_B \sim 1-2$ GeV for the baryons and $m_M \sim 0.3-1$ GeV for non-strange mesons, and appropriately higher for strange mesons and baryons. That the non-strange generic meson resonance mass should be centered near 600 – 700 MeV should be no surprise, and is consistent with our simple picture for these objects, that they comprise a constituent $q\bar{q}$ bound pair.

Produced mesons are of course not allowed to interact until a formation time τ_f has passed, this is then one *real* parameter in the model, perhaps determinable from pA, or as in earlier work from collisions of light nuclei [9]. Finally, these resonances decay by pion emission into observable π 's, ρ 's, K 's, hyperons and nucleons, and as many additional resonances as one cares to include. In this early work we limit ourselves to π 's, ρ 's and K 's. The decay time for the generic resonances constitutes a second free parameter τ_d . We will need here, even more than in cascading at the lower energies of the AGS, to use empirical knowledge of pA collisions and also perhaps light ion data to predict the most massive ion collisions.

The statement is often made that one's lack of knowledge of resonance-resonance interactions opens up to cascade models a very large well of parameters. This is emphatically not the case here. We do not treat resonance interaction cross-sections as free, but instead employ, as did Gottfried [11] a universality principle for soft interactions. Surely, for soft baryon-baryon interactions, most detailed properties of the resonances are irrelevant, with perhaps only sizes and reaction thresholds playing any role in determining the nature of the interaction, which must after all be created by multi-gluon exchange. In fact, at this point, we also ignore size differences between the resonances, with the exception of very small objects such as charmonium mesons. This limits the number of free parameters in the model to a minimum, so far just the two times τ_f and τ_d . The important proton-proton and meson-proton data, over the range of energies at which cascading takes place, are the primary input and are determined from existing experimental measurements. Baryon-meson interactions are similarly fixed from known data. Meson-meson cross-sections are normalised

to meson-baryon and baryon-baryon by appealing to constituent quark model counting.

No attempt has been made here to fit the low energy cascade smoothly onto AGS energies. The cross-sections have been followed sufficiently far down in energy, however, to ensure that the broad features of spectra at SPS and certainly RHIC energies are adequately determined within the model. In this first presentation, we focus our attention on calibrating and testing the code on known data at the CERN SPS, and give only one example of a preliminary calculation at $\sqrt{s} = 200$, Fig(4).

The material is laid out as follows. In Section II the fundamental input to the cascade, the hadron-hadron modelling, is described in detail. Section III considers the initial high energy phase and then the reinitialisation, both in nucleus–nucleus collisions. In Section IV, the final phase, a soft cascade, is described and applied to SPS data. Drell-Yan simulations are treated in Section V while Section VI presents further results, conclusions and points out future directions.

II. MODEL FOR HADRON-HADRON INTERACTIONS

The objective of the cascade approach to calculating nucleus-nucleus collisions is to proceed from a knowledge of elementary hadron-hadron collisions to a prediction of the far more complex many body event. This is, as will become clear, not completely possible in the environment of ultra-relativistic collisions. Although it may be an acceptable approximation to omit the small shell-model-like average field at the high energies we consider, it is not possible to ignore the time structure of the elementary collisions. Nor can one neglect the nature of the objects initially produced, which later rescatter during the cascade. At AGS energies [8], $E_{cm} \sim 1\text{--}5$ GeV, the introduction of the most evident, lowest lying resonances, the Δ , the N^* and the ρ , was sufficient for a reasonably accurate picture of the dynamics. The essential time scale for a many body collision was set by the resonance lifetimes, all ~ 1.5 fm/c. Since this scale was in general shorter than the ion-ion collision time τ_c , that is, the time taken for the colliding nuclei to pass through each other, most rescattering involved these resonances.

At the considerably higher energies encountered at SPS and RHIC, $\sqrt{s} = 15 - 200$ GeV, the Lorentz contraction is much more severe. The time τ_c is now comparable to (SPS), or smaller than (RHIC), both the resonance lifetimes τ_d and the meson formation time τ_f . It is therefore necessary to be guided more by experiment, in particular by pA and the lighter ion-ion cases, as well as by existing theoretical treatments of hadron reinteraction in nuclei [11,12,21]. At these higher energies we should of course also allow for the possibility of partons being freed from hadrons in collisions of high enough transverse momentum. It is nevertheless interesting to consider first a model restricted to soft collisions, including however some rare hard processes.

Many approaches [3,6,7] have been put forward to handle the reinteraction, including strings [1,2], but we prefer to retain a particle nature for the cascade. The first necessary element then is a model for the hadron-hadron system, beginning with nucleon-nucleon but easily extended to meson-nucleon and ultimately applicable to any two body hadron-hadron collision. The basic processes are elastic scattering and inelastic production of mesons. Typical samples of the cross-section fits we use are shown in Fig(8) and in Figure (9) for the

total pp scattering and inclusive Λ -K production respectively. Elastic scattering data exists over a wide range of energies for pp and in this case we fit the basic angular distributions.

We divide inelastic production into the well known categories [32]: diffractive scattering, referred to as single diffractive (SD), and non-single diffractive (NSD) scattering [31]. A graphic description of these processes is given in Fig(10). The SD process leads to a rapidity gap between one of the leading hadrons and the rest of the produced mesons, and is associated with the triple Pomeron coupling [28], while NSD production is attributed to single (or multiple) Pomeron exchange and results in the observed meson plateau at mid-rapidity. We have not made a serious effort to include the rapidity correlations also implied by the Pomeron exchange model, in the belief that these effects are very likely to be washed out in ion-ion cascading: however, no serious obstacle exists to doing so. This multiperipheral model of the soft production then represents the basis for our development, but it must be supplemented by an intermediate picture which allows us to apply it, not only to hadron-hadron interactions in free space but also inside a nuclear environment. The generic mesons depicted in Fig(10), and the generic baryons, with rather light masses selected in the ranges suggested above, constitute the basic elements for rescattering in the second-phase of the cascade. We reemphasize the $q\bar{q}$ and qqq nature of the generic resonances, structures easily related to the constituent quark models which are frequently used for discussing soft QCD physics.

A further crucial element of the hadron-hadron model is the final state meson multiplicity distribution and its energy dependence. These distributions for NSD and SD together are assumed to satisfy the KNO scaling law [30], despite deviations from scaling noted in CERN UA5 experiments at the SPS [31]. Our theoretical fits to these distributions, over a wide range of \sqrt{s} , are displayed in Fig(6) and Fig(7). These figures demonstrate the reasonably high quality of the fits. The distributions for SD scattering are taken to reproduce known measurements as discussed by Goulios [32].

Our principal phenomenological sources here are the rapidity [32] and multiplicity [33,31,34] information obtainable from the elementary collisions, generally nucleon-nucleon or pion-nucleon, but also both proton and pion-nucleus scattering. Under the umbrella of soft SD and NSD processes we include also strangeness production. Introduction of truly heavy flavours, however, should in general be done via hard processes.

Guided by our experience in cascading at the lower AGS energies, we introduce an intermediate step into the SD and NSD production: we imagine these processes are mediated by a set of intermediate generic hadron resonances. These soft, Pomeron-mediated, interactions [28,29] involve small p_T but appreciable energy loss, and hence are thought to proceed on a slow time scale, ~ 1 fm/c in the rest frame of the relevant particles. For generic mesons we include $I = 1$ (ρ -like) states with masses in a range between a minimum 300 MeV and a maximum at or near 1.0 GeV, and for simplicity a fixed width $\Gamma \sim 125$ MeV. Many of the results we obtain would equally well follow from the using a single average mass for the generic mesons near 600 MeV, in the hadron-hadron model as well as later on in AB collisions. All resonances of course eventually decay into observed stable (under strong interactions) mesons and baryons. The low masses assigned guarantee that p_T remains small in hadronic processes, even as the resonances decay.

The generic baryons are either $I = 1/2$ (N or N^* -like), or $I = 3/2$ (Δ -like), with masses restricted to the range 1–2 GeV and widths similar to those for the mesons. In addition we

include resonances analogous to the Λ , Σ and K at appropriately higher mass due to the presence of a strange quark. To reiterate, using a single, rather low excitation mass for these objects would affect the modelling very little. Though there is some freedom in the general choice of these resonance characteristics, all parameters are ultimately fixed by the known data. None of this two body information is readjusted, in nucleus-nucleus interactions; the fundamental connection with the two body measurements remains inviolate. If, for instance, we were to use a somewhat different mass range for the generic resonances, the constraint that we must describe the correct elementary multiplicity distributions would lead to a change in the number of π 's into which each generic resonance decays. These correlated changes persist also in AB collisions making the results more stable than one might imagine to changes in parameter choices for the hadron-hadron model.

In Figure 11 we display the final fits to pp at the highest energies relevant to this work [23], $\sqrt{s} \sim 20$ GeV, as well as for $p\bar{p}$ at the extreme energy of the Tevatron $\sqrt{s} = 1.8$ TeV. The fit to the total cross-section is shown in Figure 8. Similar descriptions and results are obtainable with the pion-nucleon system, and of course we avail ourselves of these in the ensuing development. The total multiplicity distributions has been adjusted to account for the presence of strangeness.

Our model of the two hadron system is very similar in philosophy to the multiperipheral models [12,13,28]. It is clear from Figure 9 and the development of this section that a central feature, the rapidity ‘plateau’ for mesons in NSD scattering, has been incorporated here. Single diffractive clusters with an observed rapidity gap are also present. One might further justify the use of intermediate state, generic mesons, by the oft described pion clustering seen in early experiments [35–37]. The generic resonances, as indicated, later decay into two or three ‘stable’ mesons, including for now π 's, ρ 's and K 's.

The most important features of the soft hadron-hadron system input for the ion-ion cascade are now set: first the energy loss, second the multiplicity distribution, and in addition the fluctuations in both of these resulting from two-body dynamics and geometry. In particular, the degree of energy loss in SD and NSD scattering is highly correlated to the width in rapidity of the final π^- distribution in Fig(11). This in turn enables a surprisingly high energy loss for protons in the rather light S+S system, in agreement with experiment. More baryons than one might expect end up at mid-rapidity in central S+S collisions [24–26].

We finish this section by restating the universality principle [8,11] we employ for in-medium resonance-resonance interactions. These cross-sections are all, aside from obvious adjustments in energy thresholds, taken equal to their free space analogues, that is they are set equal to the appropriate one of σ_{NN} , $\sigma_{N\pi}$ or $\sigma_{\pi\pi}$. This principle worked well in the cascade ARC, used at the AGS, and it has the virtue of excluding many adjustable parameters. One might well expect such soft QCD, multi-gluon exchange interactions to depend on the sizes of the initial hadrons involved, but given the narrow range of masses chosen for the generic resonances, size should not be a large factor. The $c\bar{c}$ states such as J/ψ with their characteristic small size are obviously exceptional.

III. NUCLEUS-NUCLEUS SIMULATION

One of the puzzles posed above is the apparent contradiction between the observed linear A-dependence of the production cross-section for massive Drell-Yan pairs in proton-nucleus

and nucleus-nucleus [18,25–27,20,19] scattering, and the observed energy loss [9,25–27]. The Drell-Yan process is presumably hard, rapid and describable by perturbative QCD, while meson production is mainly soft, slow and non-perturbative in nature. We now try to exploit this difference in time scales, a difference which is itself a function of collision energy, to create a global cascade incorporating both hard and soft processes. To do this we separate the simulation into two phases, connected by an overall reinitialisation. The first phase, a fast cascade, is restricted to recording the space-time geometry of the nucleus-nucleus collision, as a series of nucleon-nucleon collisions, while permitting energy loss to occur only from sufficiently rapid processes. In this work only the rare processes of Drell-Yan and charmonium production are used as examples of hard processes, and more general production of hard partons is left for future investigation. Such an approach will be sufficient to answer the most interesting present question: Can one rule out a purely hadronic explanation of charmonium suppression seen at the SPS?

A. The High Energy Cascade

The geometrical picture of the initial high-energy cascade on incoming nucleons in both target and projectile has already been shown in Fig(3). The method used here is straightforward and indeed closely resembles, in outline, an eikonal or Glauber approximation. However, the random, fluctuating nature of a cascade is retained. In each event, the collision between projectile and target is initiated with the correct energy and a nucleon configuration randomly selected within the allowable nuclear geometries. The two-body cross-sections, evaluated at the incoming energy and again employing Monte-Carlo, are used to trace out the collisions and particle trajectories in phase space. This history is later used to fix the nucleon positions in space-time as well as to calculate the energy-momentum losses. Should a hard collision intervene in the initial phase, its associated energy loss and production characteristics would also be recorded, and the energy lost would become unavailable for soft meson production. This energy, if transferred to a perturbatively interacting parton, could nevertheless reappear in the final soft cascade through hadronisation of the parton.

The time evolution of the high energy phase is completely determined by normal cascading with nucleons proceeding along straight lines between collisions. However, in the first stage only elastic collisions are allowed between nucleons (except for the rare production of a charmonium or a Drell-Yan pair), and the p_T is first fixed at zero. This of course leads to the light-cone-like structure seen in Fig(3), which as we pointed out, hopefully limits to an acceptable extent the frame dependence of the nuclear collision. One might speculate that, at least to a first approximation, ignoring the soft energy loss retains within each nucleon a coherence which is only destroyed much later.

B. Reinitialisation

We present enough of the structure of the cascade code to illustrate the information recorded and later reused. The main global data structures are a particle list and a collision list. As collisions occur they are removed from the collision list, and the particle list is rearranged, removing any particles which have collided from the active portion of the list

and adding new particles produced in the collision. In the initial, hard cascade, the only produced particles are nucleons or possibly charmonia and Drell-Yan pairs. Pointers are maintained so that after the initial hard cascade is complete (after the last high energy nucleon-nucleon collision is removed from the list), the final baryons may be easily traced back to the initial ones: this is possible since fermion lines must be continuous from the initial to the final state. In this way, the entire space-time history of the cascade is kept available as a guide to reinitialisation.

During reinitialisation a further data structure is introduced: the group list. We construct groups of nucleons in a manner described fully below. For the purpose of calculating soft energy loss nucleons in these groups are considered to have interacted coherently with one another. Into these groups we place, particle by particle, mesons carrying the lost energy. All conservation laws are enforced at the group level.

The group structure is virtually dictated by pA collisions where, given the finite range of the strong interactions and the relativistic γ 's at the SPS and at RHIC, the incoming proton collides mainly with a row of target nucleons in its direct path. A simple, symmetric, generalisation of this group structure is used for the AA case. Finally, the energy-momentum lost is transferred onto the generic mesons, whose multiplicity is fixed by the record of nucleon-nucleon collisions. There is only limited freedom in assigning the groups. Quantitatively, the possible alternatives make little difference to the results, not least of all because the second phase cascade takes place at greatly reduced energies, comparable in both SPS and higher energy RHIC collisions. In fact, the model resembles an extension of the wounded nucleon model [38]. We have essentially labelled each incoming nucleon with its multifaceted history. One might refer to this as a 'painted' or programmed nucleon model.

The group selection procedure we describe here is essentially topological in nature. At the completion of the fast cascade one selects, as a seed for the first group, that nucleon which underwent the maximal number of collisions in the hard cascade. In a first pass, one then adds, to the group containing this seed nucleon, all those nucleons with which it collided. Since we consider only the highest energy collisions in the fast cascade, these colliders are all going (in an equal velocity frame) in a direction 'opposite' to the initial seed nucleon. If the seed nucleon originates from the target, then the colliders come from the projectile, and *vice versa*. Clearly, in this way, we generally begin with nucleons near the center of the collision region, where the longest sections of target and projectile passed through each other.

Although geometry has been carefully left out of this procedure, it plays its accustomed role, since colliders are separated at most by one cross-section distance. A second pass is then made to augment and more importantly, to symmetrise the groups, kinematically speaking, between projectile and target. The collider nucleons added in the first pass are again ordered by the number of collisions they suffered, and the maximal nucleon then has its 'opposite' colliders included. The nucleons so included have all interacted with each other and are separated transversely by at most two cross-section distances. This completes the first group. A schematic representation of a group constructed in this way is given in Fig(5).

One then proceeds similarly for the next group, and so on, until all possible nucleons have been assigned to groups. At this point there may yet remain some 'orphaned' interacting nucleons, which have interacted but have not been assigned to any group, and possibly also some spectator nucleons, which have not had any collisions at all. The 'orphans' are assigned

to groups at random, by searching the existing groups for a nucleon with which they have collided. Finally, non-interacting particles are left individually as spectators.

This method coincides with the natural definition of an interacting group in pA collisions. It also leads to groups of reasonable size in both very massive (Pb+Pb) and lighter (S+S) ion collisions. For example, there are some 46 groups produced in very central Pb+Pb at the SPS with the largest group containing 25 or so nucleons. The groups generally decrease in size, as one progresses towards the edges of the interacting region. In a typical central Pb+Pb event we find as many as ten spectators, whose history is then self-evident. In central S+S there are of course fewer and smaller groups. The rest of the calculations in this section are carried out in the individual group rest frames, after appropriate boosts from the preselected global frame. Finally, these results are boosted back to the global frame to and used to initialise the final low energy cascade.

The energy-momentum loss for each nucleon is tied to its collision history, by reconstructing for each collision it had, using the basic elementary NN model of Section II, the specific energy loss and the type and multiplicity of mesons produced. For example, strangeness production, both associated $\Lambda - K$ and $K - \bar{K}$, is allowed and is significant at the SPS. A maximum rapidity for the generic mesons is assigned, again related to that found in the basic pp interaction, but the final y distribution of mesons within a group is then mostly dictated by energy-momentum conservation. Transverse momentum is added for the baryons assuming a random walk occurs, with step size δp_T taken from basic pp collisions. The total meson transverse momentum must cancel that in the baryons. A simple Gaussian parameterisation is used for the meson phase space in p_T . Particular problems of course occur at the edges of phase space in rare events and these were solved on a case by case basis.

We now describe the method of tracing the collision history of a particular baryon. The total number of collisions that a given baryon suffered in the hard cascade is already known: the first of these naturally takes place at the maximum initial energy. The ratio of elastic to inelastic scattering, as well as the multiplicity, and type, of mesons created in a nucleon-nucleon collision follow from our KNO scaling distributions (Figures 5-6) and cross-section fits. The baryon, in each successive collision, is given a choice of all possibilities, beginning with elastic or inelastic scattering, the latter divided into SD, NSD and a small absorptive probability for high collision number. If an inelastic collision occurs, energy is removed from the baryon.

These choices are carried out in an effective two-body frame, determined by searching through the group for the highest energy remaining two-nucleon collision energy involving the nucleon under consideration. The average energy loss for baryons, is calculated from the input pp interaction and multiplicity distributions. At high energies there is a rough rule of thumb in pp collisions, stating that approximately one-half the energy is lost in the center of mass frame. This fixed downward drift in rapidity $\Delta y \sim 0.6 - 0.7$ cannot continue to arbitrarily low energy collisions, but must be severely limited when low y is achieved. This is accomplished by adjusting a Gaussian parameterisation to produce a scaled drift in rapidity, with gradually decreasing Δy at large collision numbers.

The end result in a given group is a set of baryons with fixed 4-momenta, positions and also a set of mesons, of specific charges and flavours. There remains the problem of depositing the implied longitudinal energy-momentum lost from the baryons onto the generic mesons. If life were simple this would be a single procedure. In fact to satisfy the final phase space

requirement, energy-momentum conservation in the group, one must allow for some further readjustment of the baryon momenta with due attention paid to very high multiplicity cases. In such a case, where the initial attempt to distribute the energy-momentum among the mesons fails because not enough energy is available for the mesons, baryon momenta already assigned may be rescaled. Multiplicity and p_T may also be readjusted in extreme cases to yield the desired solution.

Finally, the mesons and baryons in a group are transformed back to the preselected global cascade frame. Other alternatives we pursued for constructing groups and treating phase space, altered the quantitative results rather little, once sensible solutions were found, so we are reasonably confident the model is stable. The intricacies of phase space selection are very strongly dictated by overall energy-momentum conservation, once the final multiplicity and average p_T is known, and thus the reinitialisation is again quite robust. Guidance from the elementary hadron-hadron data is clearly vital. Fig(12) and Fig(13) display reinitialised rapidity spectra for both meson and baryon generic resonances.

The final step in the reinitialisation is to place all of the mesons and baryons on a new initial spacelike surface, which we take to be the surface $t = \tau_c$ in the global cascade frame. That is, the second stage, soft cascade starts at the time of the last nucleon-nucleon collision which occurred in the initial stage. It was thought best to distribute the mesons produced in a group randomly (that is, uniformly) along the space-time paths followed by the baryons in that group during the initial cascade (see Fig(3)). Any sins committed in making such a somewhat arbitrary choice are clearly and strongly remediated, since in any case a formation time must elapse for each meson before it can actually interact. Figure 14 displays the mesons after the passage of the formation time, for Pb+Pb at 158 GeV/c, in the z - t plane. A limited variation in the initial space-time placement of generic mesons, at the end of the fast cascade, produces rather insignificant changes in the final spectra. The four-momenta, in the global frame, and final positions of the baryons are already known from the first stage. We then restart the cascade by constructing all possible two body collisions and decays among the meson and baryon resonances produced in the hard cascade.

An important first approximation to keep in mind is that many of the results of the fast cascade as described here are, for the baryons, similar to those expected from a pure Glauber theory calculation. This point will be made more evident in later work on J/ψ production in pA and AB collisions.

IV. LOW ENERGY CASCADE

The final stage of the cascade involves standard two-body hadron-hadron collisions and is carried out for the most part similarly to, for example, the low energy cascade ARC [8]. However, our model of hadron-hadron scattering and phase space, as described above, differs significantly and is in fact necessary at the much higher energies encountered at the SPS and RHIC. We are employing as rescatterers the generic resonances defined earlier, for both mesons and baryons. The cross-section tables are defined to low enough energies, and proper thresholds are included for eventual production of the observed low lying resonances. Only those meson resonances likely to significantly affect the dynamics are included at this stage, i.e. the π and the ρ . Almost without exception the ensuing collisions at SPS occur

at relatively low center of mass energies, $\sqrt{s} \sim 5 - 8$ GeV. The final second phase cascading can truly be labelled as ‘low energy’.

Additional aspects requiring discussion involve the role of the produced particle formation time τ_f and of course the decay time τ_d of the generic hadrons into final state mesons. These certainly involve parameters not easily discernible from elementary hadron-hadron measurements. Some attempts to use HBT for determining the size of interaction regions [39] in these elementary collisions might, however, be viewed in this light. The formation time is a straightforward, often used concept, and in accordance with most estimates we take $\tau_f \sim 1$ fm/c, with some 0.25 fm/c attributable to the initial rapid phase at SPS energies. The generic resonances have rather low mass and are allowed to decay into only two or three π 's (and/or strange mesons if strangeness is present), Given the low values and narrow range of masses for the resonances we have, as indicated, opted to use a single, constant decay width, $\Gamma = 125$ MeV. This choice does not affect the results in any dramatic fashion.

We intend in future to use both pA and light ion systems to finally fix the formation and decay times. We choose to accomplish this here by focusing on the S+S data collected by NA35 [25], leaving more complete discussion of pA to future work. In earlier work [9], the decay constant played a significant role in normalising the pion spectrum for S+S. The extrapolation to Pb+Pb, using of course the same decay time, then proved reasonably successful [9], indicating that the treatment of energy loss in the earlier work had some merit. This helped define one side of the fast vs. slow energy loss dilemma we posed at the outset. The large influence of the decay time in the early calculation was easily understood. Lengthening this time delayed the reinteraction of produced particles until particle densities had decreased through expansion of the entire interacting system. This led in turn to a lower pion yield. The reduced dependence on these times, seen in the new double cascade can be attributed, once again, to the lower average collision energies in the final phase.

The initial particle list for the soft cascade, including space-time coordinates and four-momenta of all mesons and baryons were set in the reinitialisation. Their rapidity distributions and the initial geometry, are depicted in figures (4), (11), (12) and (13). A major reason for the lower final collision energies is that rarely do particles originating separately from the initial target and projectile configurations meet. Spectators also avoid each other for geometric reasons, arising as they do, from regions of low nucleon density in the hard cascade. The results of the low energy cascade, for a range of CERN SPS energies, are displayed in a series of figures (14–17) for the S+S and Pb+Pb systems. These results of course represent the output of both stages of the cascade, and wherever possible are compared to existing data. The theoretical description of the experiments is certainly acceptable. The proton distributions, for S+S in Fig(15) and for Pb+Pb in Fig(16), measured by the ‘ $h^+ - h^-$ method’ [25,26], show a large energy loss, perhaps close to saturation, as suggested by the experimentalists [24] for central collisions in the light S+S system.

The corresponding pion spectra in S+S and Pb+Pb are well reproduced by this (Lucifer II) simulation, both in magnitude and shape. There is, however, still a necessity for better experimental determination of both proton and pion spectra at midrapidity in Pb+Pb at the SPS. An appreciable increase or decrease in energy loss and meson number in the central region could have a commensurate effect on the very interesting question of the degree of charmonium breakup expected during the soft cascade, i.e. the amount of J/ψ suppression attributable to comovers.

Moreover these S+S and Pb+Pb results are achieved using the same parameters for both systems; only the dependence on the number of first stage baryon-baryon collisions plays a distinguishing role in reinitialisation. The average number of hard collisions per nucleon in central S+S is near 3.5, while in Pb+Pb it is closer to 7.5, with wide fluctuations about these averages seen in both nuclear systems. Despite this difference in average hard collision number one can begin to understand the saturation of stopping referred to by the experimentalists [24–26]. At high energy considerable energy is lost, perhaps one-half of the total, per nucleon-nucleon collision and there is very little left to lose after just a few collisions. Nevertheless the final soft cascading does rearrange and broaden the rapidity distributions, even if it does not add much to the production of a given species.

V. DRELL-YAN

Here we present briefly the method used for calculating the other, important side of the quandary we faced at the start: the production of massive lepton pairs. We limit ourselves to the canonical FNAL E772 pA measurement at 800 GeV/c, but in fact the method of calculation guarantees agreement with the lower energy pA and AA data collected by NA50 [27]. The calculation is straightforward and is a first example, for us, of a hard process added to the initial high energy cascade. Drell-Yan is generally considered perturbatively calculable for dilepton pairs with masses $M_{\mu\mu}$ in excess of 4 GeV. We have simply used the first Born approximation for the production in NN , $N\pi$ and $\pi\pi$, with a multiplicative factor for p_T dependence and structure functions taken from early papers on the subject [18]. Our concern here is mainly with the overall A -dependence of the process, so that including precise Q -factors, higher loop corrections to the p_T distributions, and using the most current structure functions, are all unnecessary complications. We find that contributions to Drell-Yan from meson-nucleon and meson-meson collisions, present in the second low energy phase, are completely negligible at CERN energies. Only the high energy nucleon-nucleon collisions in the first phase count.

The calculation is straightforward: production in the short time defined by such high mass pairs proceeds essentially without energy loss, since it is extremely rare, and occurs during the initial Glauber-like hard cascade. The simulation produces the points shown in Fig(20), which depicts the A -dependence of the pair yield, after division by A . The E772 [19] measurements suggest a strict proportionality, $\sigma_{DY} \sim A$. To perform the Drell-Yan microscopically we have introduced parton structure functions [18] and the requisite parton variables, into the coding. But the theoretical results in Fig(20) could have been obtained purely geometrically from the elementary production rates and from the space-time history of the first, high energy, nucleon-nucleon cascade.

VI. FURTHER RESULTS AND CONCLUSIONS

The main purpose of this manuscript has been to present the theoretical underpinnings of a modified cascade simulation of high energy heavy ion collisions that can reasonably describe two seemingly contradictory aspects of the data. The observed A -dependence of cross-sections for high mass Drell-Yan production in proton-nucleus and ion-ion collisions

at SPS energies and above, suggests that high mass lepton pairs are produced by nucleons which *do not experience energy loss* during the ion-ion collision, while the observed meson and baryon spectra make it all too clear that energy is indeed lost from the baryons and goes into producing soft mesons. A standard two-body cascade model cannot easily reconcile these facts, since energy is necessarily lost with each successive two-body collision. We have suggested a solution to this quandary: the simulation should be done in three steps. First a short-time high energy Glauber-like cascade is carried out among the nucleons involving only energy loss resulting from high momentum transfer processes. This builds in the basic space-time geometry of the ion-ion collision. Second the cascade is reinitialised, allowing for soft meson production from the nucleons. This production is done coherently, from groups of interacting nucleons, but two-body inputs are used together with the collision history to strongly constrain the meson production. Finally, an ordinary low energy two-body cascade is carried out among all the particles produced in the first two stages. This modified cascade approach becomes essential at collision energies near and above those attained at the SPS, where the total time for the nuclei to pass through each other (in an equal velocity frame) becomes comparable to the time for soft meson formation ($\tau_c \sim \tau_f \sim 1$ fm).

We did not present here an inclusive treatment of all existing data, but limited ourselves to a few applications selected from CERN SPS [25,26], UA5, FNAL [23,19] experiments, to demonstrate that the ideas can work in practice. Some of these examples are from pA collisions and some from AA. In addition to the rapidity distributions for S+S and Pb+Pb, we have also considered transverse momentum distributions; examples are shown in Fig(17) for protons from Pb+Pb in central rapidity slices and also for Λ 's in comparison to recent preliminary data from Quark Matter '96 [26]. The calculated and measured 'temperatures' are in reasonably good agreement.

Nevertheless, the degree of proton stopping [24] is clearly important to our model and a better understanding of the data might point to differences between theory and experiment, heralding collective effects. It will be particularly important to see the differences occasioned by the introduction of partons. Results of parton cascades such as that of K. Geiger [40], when compared to our preliminary calculations for central Au+Au collisions at RHIC energy, suggest remarkably similar spectra may result for the mesons when partonic hard scattering and splitting processes are included. This perhaps suggests that two-body processes and energy conservation, not thermodynamics, dominate such production. Despite this, the energy and number densities for both baryons and mesons achieved in the present simulations (LUCIFER II) are high enough, $\rho_E \sim 3 - 5$ GeV/fm³, and last for sufficiently long times in central Pb+Pb collisions at 158 GeV/c, perhaps to expect unusual high density behaviour to occur. The striking new results of NA50 [27] must then be taken very seriously.

We have also considered the leading particle behaviour for pp and p+Pb, and illustrate these in a comparison with 100 GeV/c FNAL measurements [17] of proton and pion spectra in Feynman x in Fig(19). A key feature in understanding this low p_T data is the narrower transverse momentum present in both elastic and inelastic components in the NN model for Feynman x close to 1. Although these results are perhaps related to the parton structure of the proton, a simple conclusion is that the nucleon-nucleus data follows from nucleon-nucleon.

The very interesting case of charmonium production in both pA [19] and AA [27,41,42], should receive some mention. We have already treated the pA charmonium production in a

somewhat different fashion [9], following suggestions by Gottfried [11]. The model we used [9] treated the charmonium states as coupled channels, at least to the extent that the final χ states, or some pre-resonant form of them [41], are much more abundantly produced than the J/ψ . Certainly the χ states feed strongly into the ψ by electromagnetic decay. The parameters in such a model are the breakup cross-sections of the charmonium states in the initial pure nucleon cascade. The very similar suppression in pA found for ψ' and ψ by the FNAL E772 experiment [19] can perhaps be understood if one takes the coupled channels approach seriously and ties the breakup probability to the size of the charmonium state, since both the χ and ψ' are considerably larger than the J/ψ . In any case we will separately present a calculation of charmonium yields based on the current modelling.

It has of course been the principal thrust of this work to create a unified dynamic approach to calculating ion-ion collisions at very high energy, incorporating both hard processes such as Drell-Yan and the slower processes responsible for energy loss and soft meson production. So far, this has been done allowing rescattering only via hadronic intermediate states. No partons have yet been explicitly included, except insofar as structure functions must be used for the calculation of Drell-Yan production. This approach proves to be phenomenologically viable and leads to a reasonable description of a broad range of results obtained at the SPS. A secondary justification for constructing such a pure hadronic calculation is to investigate the conclusions of Kharzeev and Satz [41], namely that a purely hadronic explanation of the J/ψ suppression seen by NA50 is not possible.

ACKNOWLEDGMENTS

The authors are of course grateful to all of the experimentalists at the AGS, SPS, ISR and FNAL, who have over the years gathered the basic data. Certainly the code could not have been constructed without it. We also wish to thank Y. Dokshitzer, A. H. Mueller for instructive conversations and advice. This manuscript has been authored under US DOE contracts No. DE-FG02-93ER407688 and DE-AC02-76CH00016.

-
- [1] B. Andersson, G. Gustafson, G. Ingelman, and T. Sjostrand, *Phys. Rep.* **97**, 31 (1983); B. Andersson, G. Gustafson, and B. Nilsson-Almqvist, *Nucl. Phys* **B281**, 289 (1987).
 - [2] J. Ranft and S. Ritter, *Z. Phys.***C27**, 413 (1985); J. Ranft *Nucl. Phys.* **A498**, 111c (1989); A. Capella and J. Tran Van, *Phys. Lett.***93B**, 146 (1980) and *Nucl. Phys***A461**, 501c (1987); K. Werner, *Z. Phys. C* **42**, 85 (1989).
 - [3] X. -N. Wang and M. Gyulassy, *Phys. Rev.* **D44**, 3501 (1991).
 - [4] D. Boal, *Proceedings of the RHIC Workshop I*, (1985) and *Phys. Rev.* **C33**,2206 (1986); K. J. Eskola, K. Kajantie and J. Lindfors, *Nucl. Phys.* **B323**, 37 (1989).
 - [5] K. Geiger and B. Mueller *Nucl. Phys.* **B369**, 600 (1992); K. Geiger *Phys. Rev.* **D46**, 4965, and 4986 (1992); K. Geiger, *Proceedings of Quark Matter '83*, *Nucl. Phys.* **A418**, 257c (1994); K. Geiger, *Phys. Rev.***D51**, 2345 (1995).

- [6] H. Stoecker and W. Greiner, *Phys. Rep.* **137**, 277 (1986); R. Mattiello, A. Jahns, H. Sorge and W. Greiner, *Phys. Rev. Lett.* **74** 2180, (1995).
- [7] H. Stoecker, *Proceedings, RHIC Summer Study'96 and references therein.*
- [8] Y. Pang, T. J. Schlagel, and S. H. Kahana, *et al*, *Phys. Rev. Lett* **68**, 2743 (1992); S. H. Kahana, D. E. Kahana, Y. Pang, and T. J. Schlagel, *Annual Reviews Of Nuclear and Particle Science*, **46**, (1996), (ed. C. Quigg).
- [9] D. E. Kahana, *Proceedings, RHIC Summer Study'96*, 175-192, BNL, July 8-19, (1996).
- [10] K. Eskola, *Proceedings, RHIC Summer Study'96*, 99-110, BNL, July 8-19, (1996).
- [11] K. Gottfried *Phys. Rev. Lett.* **32**, 957 (1974); and *Acta. Phys. Pol***B3**, 769 (1972).
- [12] J. Koplik and A. H. Mueller *Phys. Rev.* **D12**, 3638 (1975).
- [13] A. H. Mueller *Proceedings, RHIC Summer Study '96*, 385-390, BNL, July 8-19 (1996).
- [14] A. Schwimmer *Nucl. Phys.* **B94**, 44 (1975).
- [15] J. D. Bjorken, *et al*, *Phys. Rev.* **D27**, 140 (1983).
- [16] Yu. L. Dokshitzer *Proceedings, RHIC Summer Study'96, and references therein.*
- [17] D. S. Barton *et al.*, *Phys. Rev.***D27**, 2580 (1983); W. Busza *et al*, *Phys. Rev. Lett.***34**, 836 (1975); W. Busza *Proceedings of Quark Matter'83*, *Nucl. Phys.* **A418**, 635c (1984).
- [18] NA3 Collaboration; J. Badier *et al.*, *Zeit. Phys.* **11**, 604, (1981); NA3 Collaboration; J. Badier *et al.*, *Zeit. Phys.* **20**, 101, (1983).
- [19] E772 Collaboration; D. M. Alde *et al.*, *Phys. Rev. Lett.* **66**, 133, (1991).
- [20] NA51 Collaboration; A. Baldit *et al.*, *Phys. Lett.* **B332**, 244, (1994).
- [21] Jianwei Qiu and G. Sterman *Proceedings, RHIC Summer Study'96* 85-90, BNL, July 8-19, (1996).
- [22] K. Geiger, *Proceedings, RHIC Summer Study'96*
- [23] Y. Eisenberg *et al* *Nucl. Phys.***B154**, 239 (1979)
- [24] J. W. Harris, In proceedings of the 12th Winter Workshop on Nuclear Dynamics, Snowbird, Utah (1995):
- [25] J. Baechler for the NA35 Collaboration, *Phys. Rev. Lett.***A461**, 72 (1994); S. Margetis for the NA35 Collaboration, *Snowbird 1994, Proceedings, Advances in Nuclear Duynamics*, 128-135, 1994
- [26] T. Wienold and the NA49 Collaboration; In Proceedings of Quark Matter '96, *Nucl. Phys.* **A610**, 76c-87c, 1996; P. G. Jones and the NA49 Collaboration; In Proceedings of Quark Matter '96, *Nucl. Phys.* **A610**, 76c-87c, 1996; T. Alber *et al.*, the NA50 Collaboration, *Phys. Rev.* **C75**, 3814, 1995; J. Baechler for the NA35 Collaboration, *Phys. Rev. Lett.***A461**, 72 (1994); S. Margetis for the NA35 Collaboration, *Snowbird 1994, Proceedings, Advances in Nuclear Duynamics*, 128-135, 1994.
- [27] M. Gonin, for the NA50 Collaboration, *Proceedings of Quark Matter '96, Nucl. Phys.* **A610**, 404c-417c, 1996; also in Proceedings of RHIC'97, BNL, July 7-15, 1997.
- [28] V. N. Gribov, B. L. Joffe and I. Ya. Pomeranchuk, *Sov. J. Nucl. Phys.***2**, 549(1966); V. N. Gribov, *JETP***26**, 414 (1968); J. Kogut and L. Susskind, *Phys. Rep***8C**, No. 2 (1973); H. D. Abarbanel, J. D. Bronzan, R. L. Sugar and A. L. White, *Phys. Rep***21C**, No. 3 (1975); H. Chen and T. T. Wu *Phys. Rev. Lett***24**, 1456 (1970).
- [29] G. Alberi and G. Goggi, *Phys. Rep***74**, No. 1, (1981), 1-207; P. V. Landshoff and O. Nachtmann, *Z. Phys.***C35**, 405 (1987).
- [30] Z. Koba, H. B. Niesen and P. Olesen, *Nucl. Phys.***B40**, 317 (1972).
- [31] G. Ekspong for the UA5 Collaboration, *Nucl. Phys.***A461**, 145c (1987); G. J. Alner for the

- UA5 Collaboration, *Nucl. Phys.***B291**, 445 (1987).
- [32] K. Goulios, *Phys. Rep***101**, No. 3, (1983), 169-219.
- [33] V. Blobel et al., *Nucl. Phys.* **B111**, 397 (1976); V. Blobel et al., *Nucl. Phys.* **B69**, 454 (1974).
- [34] CHLM Collaboration, *Nucl. Phys.***B108**, 1 (1976); J. W. Chapman *et al Phys. Rev. Lett.***32**, 257 (1973); T. Kafka *et al Phys. Rev.***D16**, 1261 (1977).
- [35] W. Beusch, *Acta. Phys. Pol***B3**, 1679 (1972).
- [36] E. L. Berger and G. C. Fox, *Phys. Lett* **47B**, 162 (1973).
- [37] A. Wu. Chao and C. Quigg, *Phys. Rev.***D9**, 2016 (1974).
- [38] A. Byalas et el., *Nucl. Phys.***B111**, 461 (1976).
- [39] R. Hanbury-Brown and R. Q. Twiss, *Nature*(London), **178** 1046 (1956); G. Goldhaber, S. Goldhaber, W. Lee, and A Pais, *Phys. Rev.* **120**, 300 (1960).
- [40] Private communication.
- [41] D. Kharzeev and H. Satz, In Proceedings of Quark Matter '96, *Nucl. Phys.* **A610**, 76c-87c, (1996).
- [42] S. Gavin, Proceedings, RHIC Summer Study'96; S. Gavin and R. Vogt *Proceedings of Quark Matter '96*, Heidelberg, May 1996.

Drell–Yan: A–Dependence

p+A @ 800 GeV/c E772 FNAL

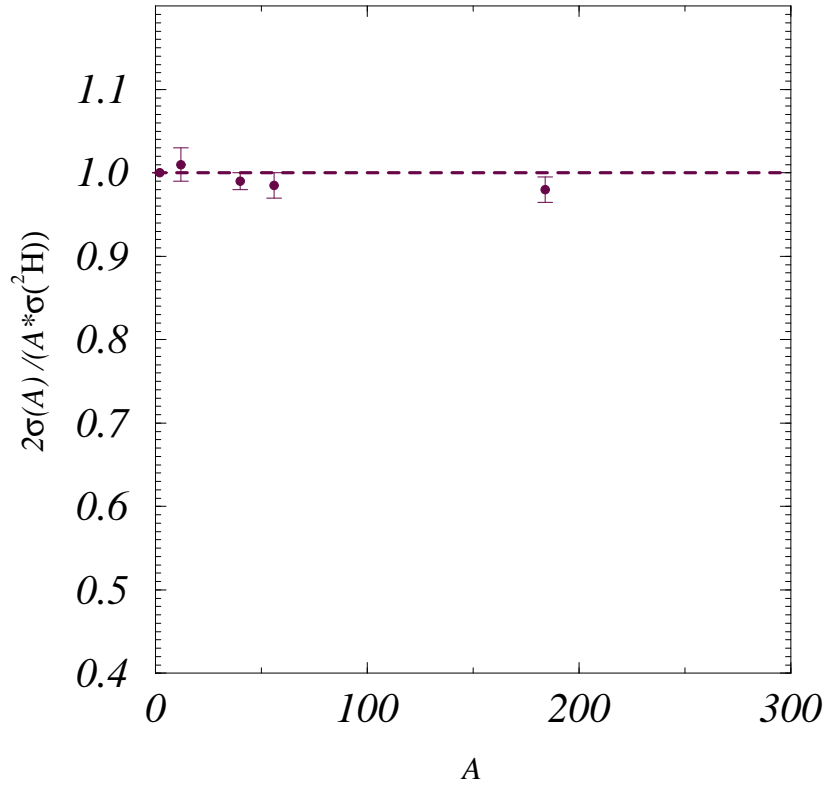


FIG. 1. The A-dependence of measured Drell-Yan from E772 (FNAL).

LUCIFER I: Pure Soft Cascade vs NA49

$Pb+Pb @ s^{1/2}=17.2 \text{ GeV NA49 (1995)}$

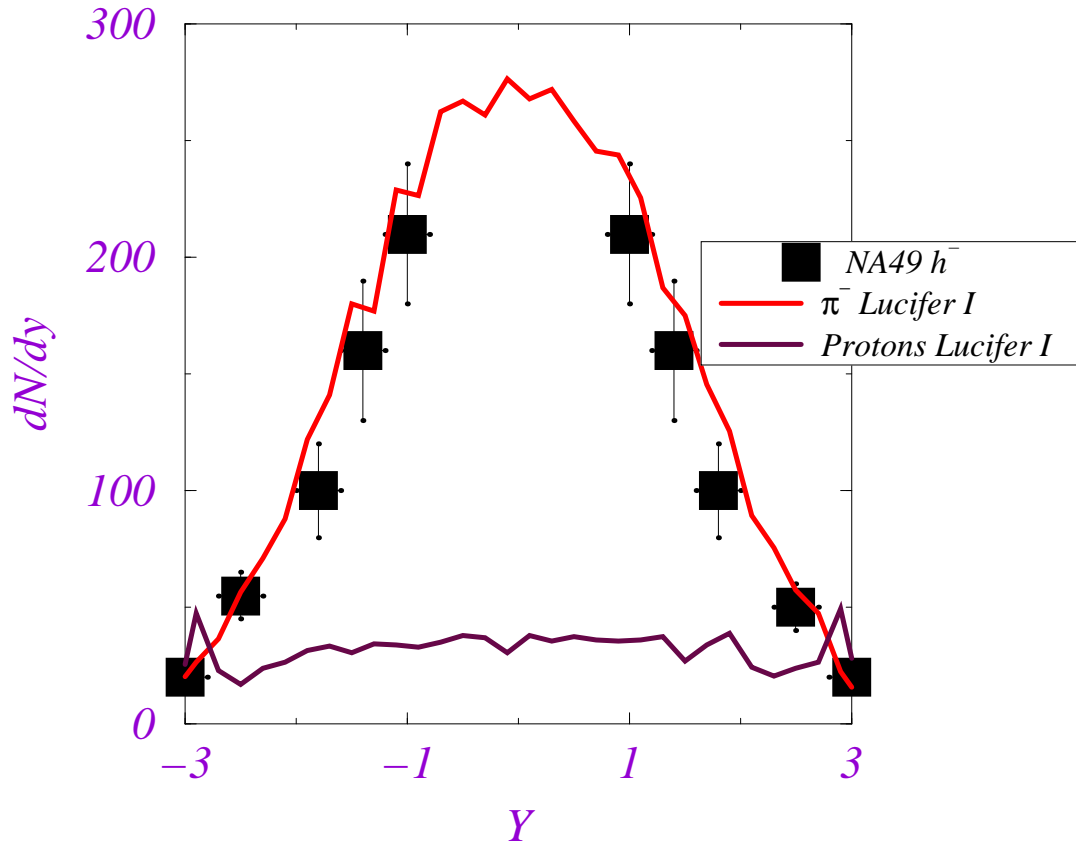


FIG. 2. Pb+Pb @ 158 GeV/c; Experiment (preliminary NA49, 1995) for Pb+Pb vs standard cascade theory Lucifer I, from RHIC'96

Baryon Final Positions (After First Stage Cascade)

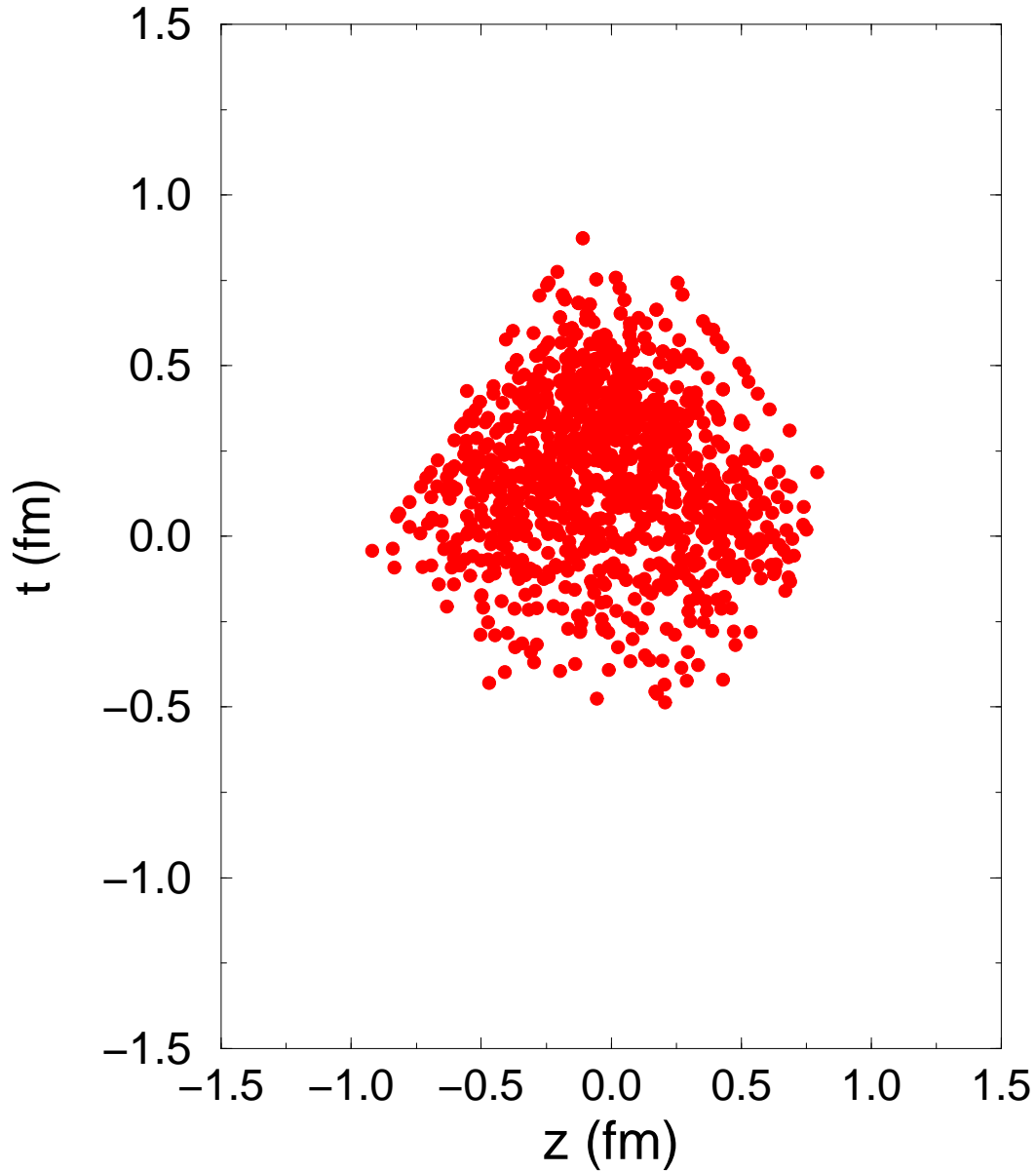


FIG. 3. Positions of baryons in Pb+Pb after first phase: Fast cascade. The time and longitudinal envelope indicates where the purely baryonic system reaches after the two massive nuclei pass through each other at this SPS energy.

Frame Dependence: Worst Case Scenario

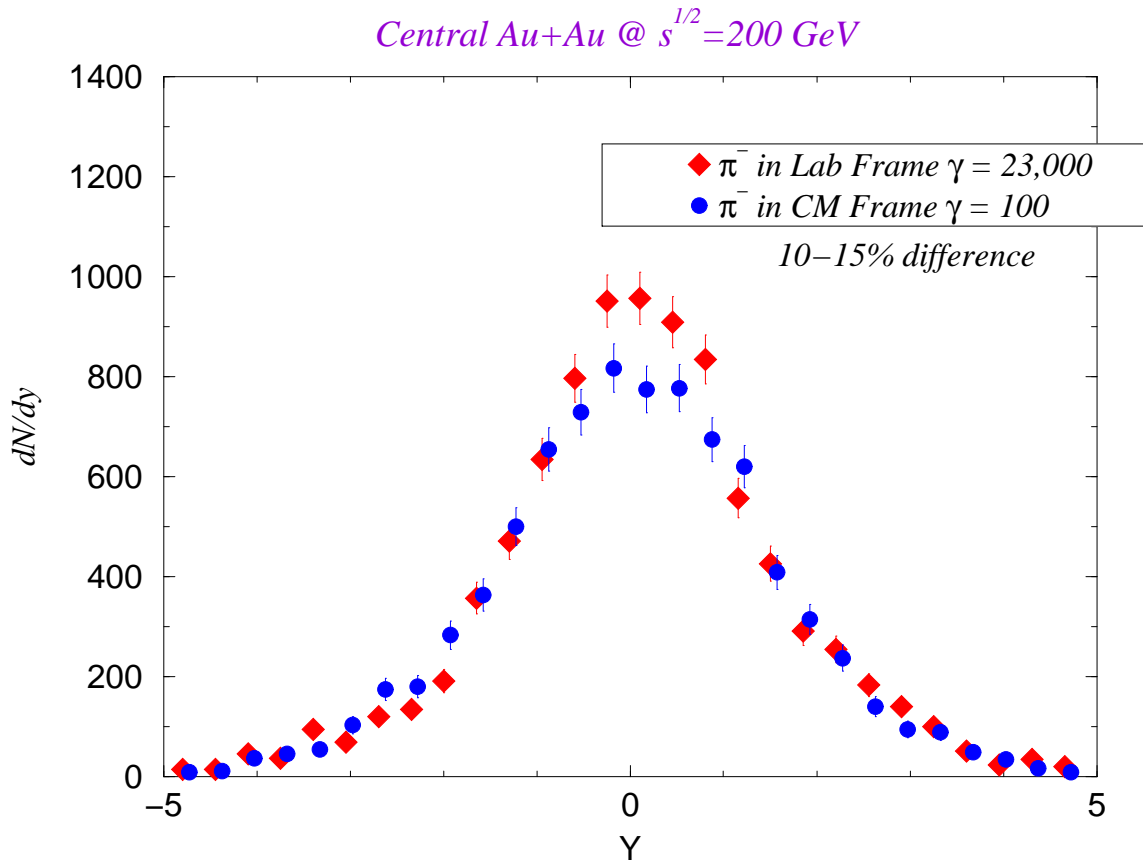


FIG. 4. A worst case scenario for frame dependence: comparison of spectra for a $b=0$ Au+Au collision at RHIC. The results are from a very preliminary calculation with LUCIFER II and do not represent a prediction, but only serves to indicate the greatly reduced frame dependence. At the SPS the dependence is within statistical errors.

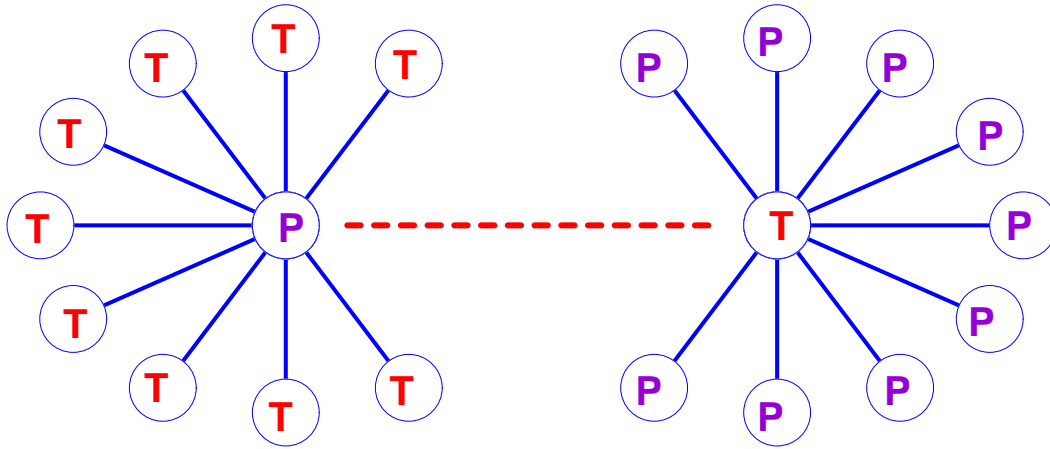


FIG. 5. A schematic diagram of the structure of the groups used in reinitialisation of the cascade. Circles inscribed with P stand for projectile nucleons, circles with T stand for target nucleons. Lines connecting nucleons indicate that they have collided in the initial cascade. A group is constructed by first finding a seed nucleon with a maximal number of collisions in the hard cascade, here represented by one of the two circles connected by a dotted line. For example, the seed might be the projectile nucleon at the left of the dotted line. All target nucleons which collided with the seed would be added to the group. In a general nucleus-nucleus collision there would be one among all those target nucleons added which suffered the largest number of collisions (here drawn at the right of the dotted line). This nucleon would in turn be used as a second seed, to symmetrise the group. All projectile nucleons which collided with the secondary seed would also be added to the group. In an actual example the groups could of course be larger or smaller than depicted here, and possibly less symmetric, depending on the relative sizes of the projectile and target, and the particular geometry of the collision.

Fit to pp Multiplicity Distribution

KNO scaling: $sd + nsd: s^{1/2} = 546 \text{ GeV}$

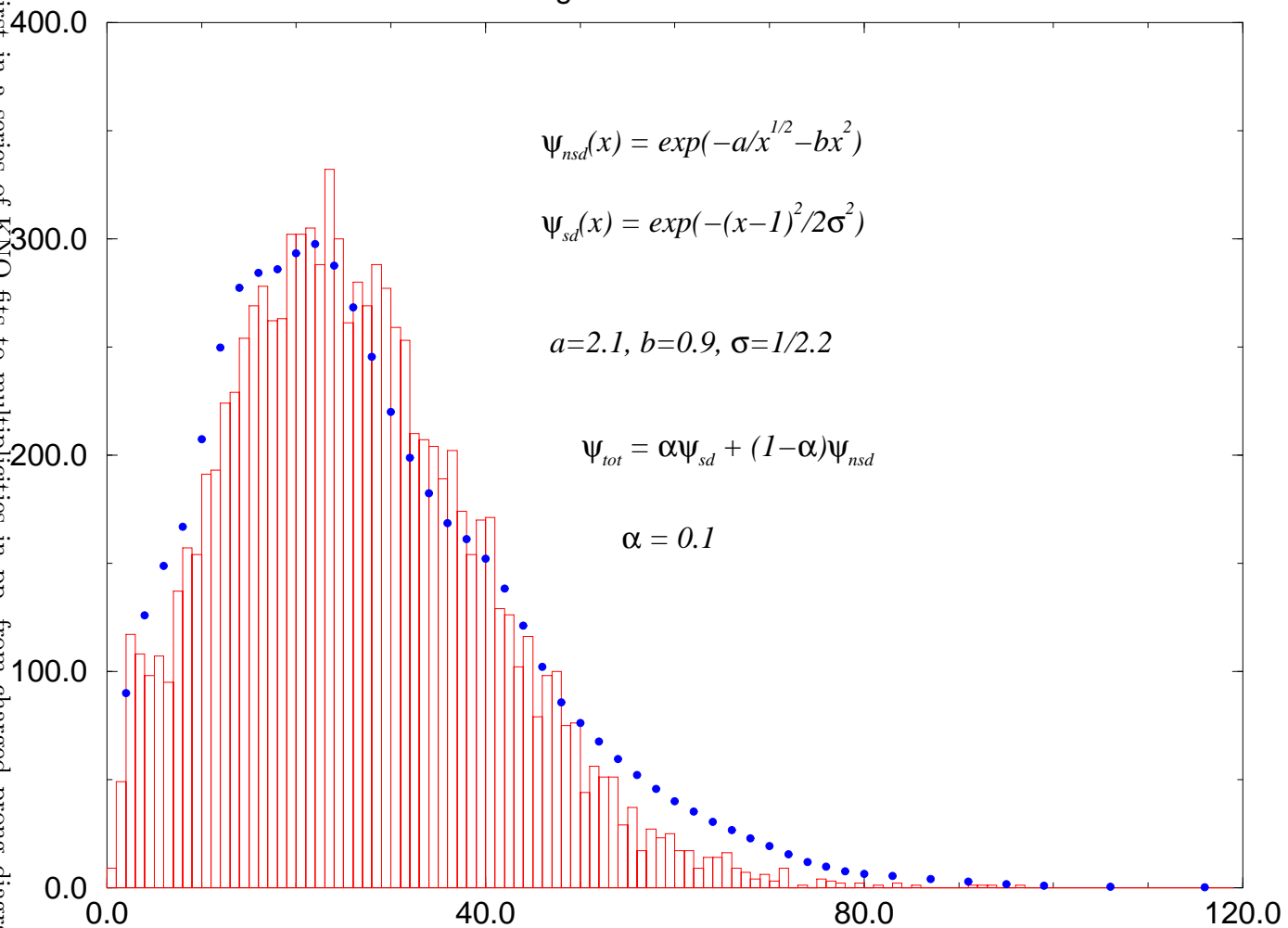
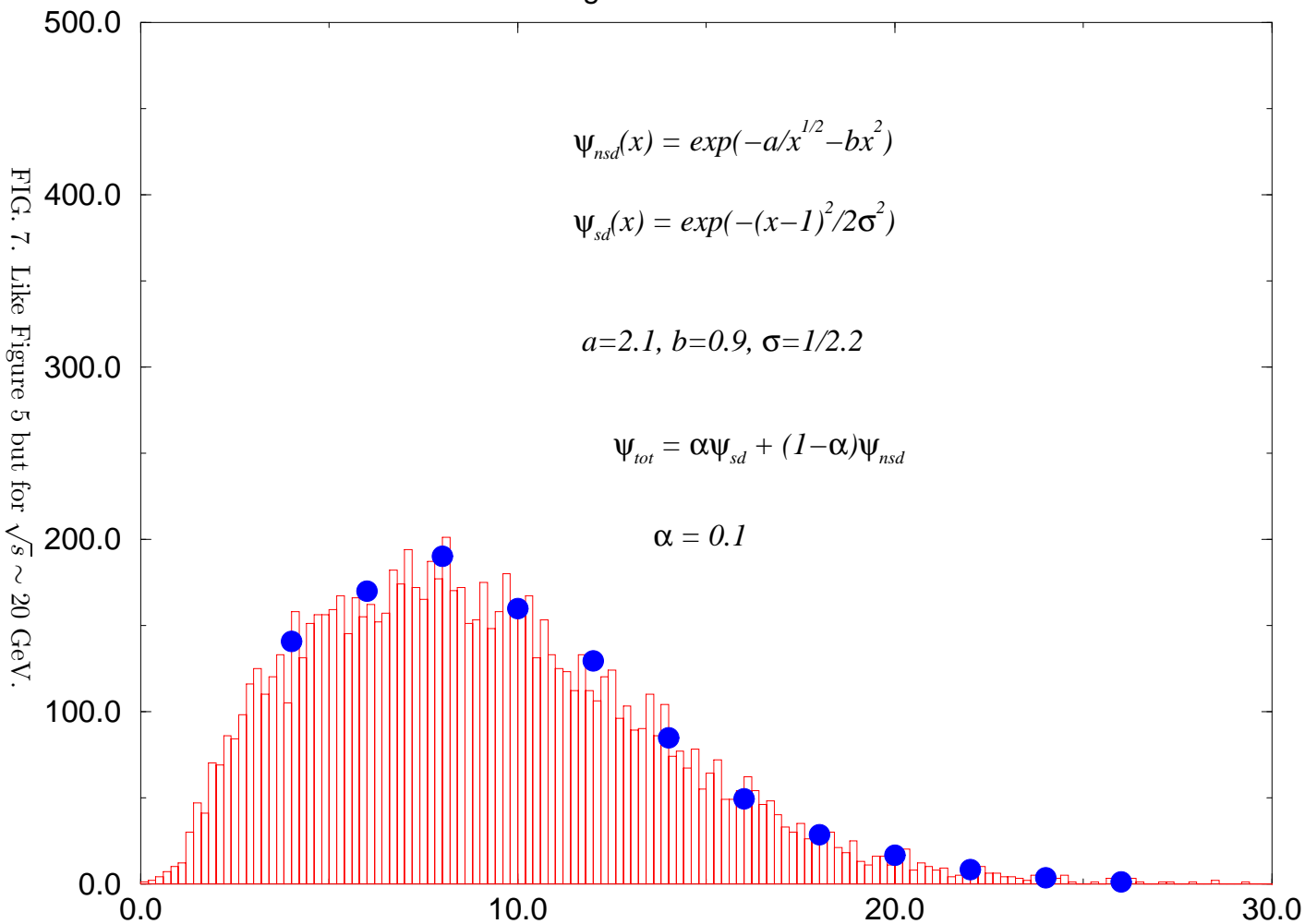


FIG. 6. First in a series of KNO fits to multiplicities in pp, from charged prong diagrams at several energies. This depicts the $\sqrt{s} = 546 \text{ GeV}$ fit and contains the particular choice of KNO function and parameters used.

Fit to pp Multiplicity Distribution

KNO scaling: $sd + nsd: s^{1/2} = 26.0 \text{ GeV}$



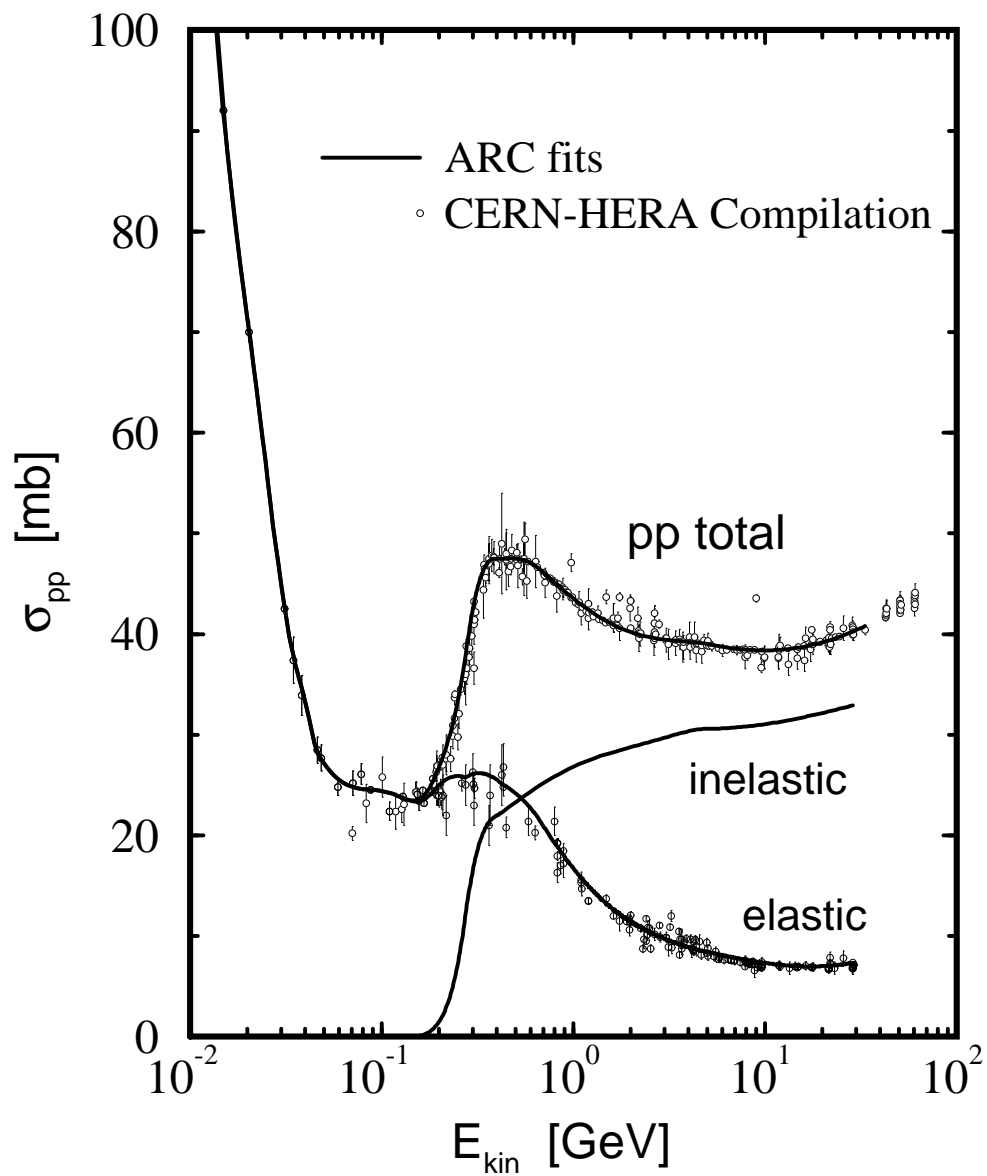


FIG. 8. Total Cross-section for pp. Experimental points for pp extends well beyond the CERN SPS energies, but above one must use $p\bar{p}$ measurements. We show only the calculated cross-section beyond the actual pp measurements

ΛK Production Cross-Section

Possible Lucifer fit vs Data

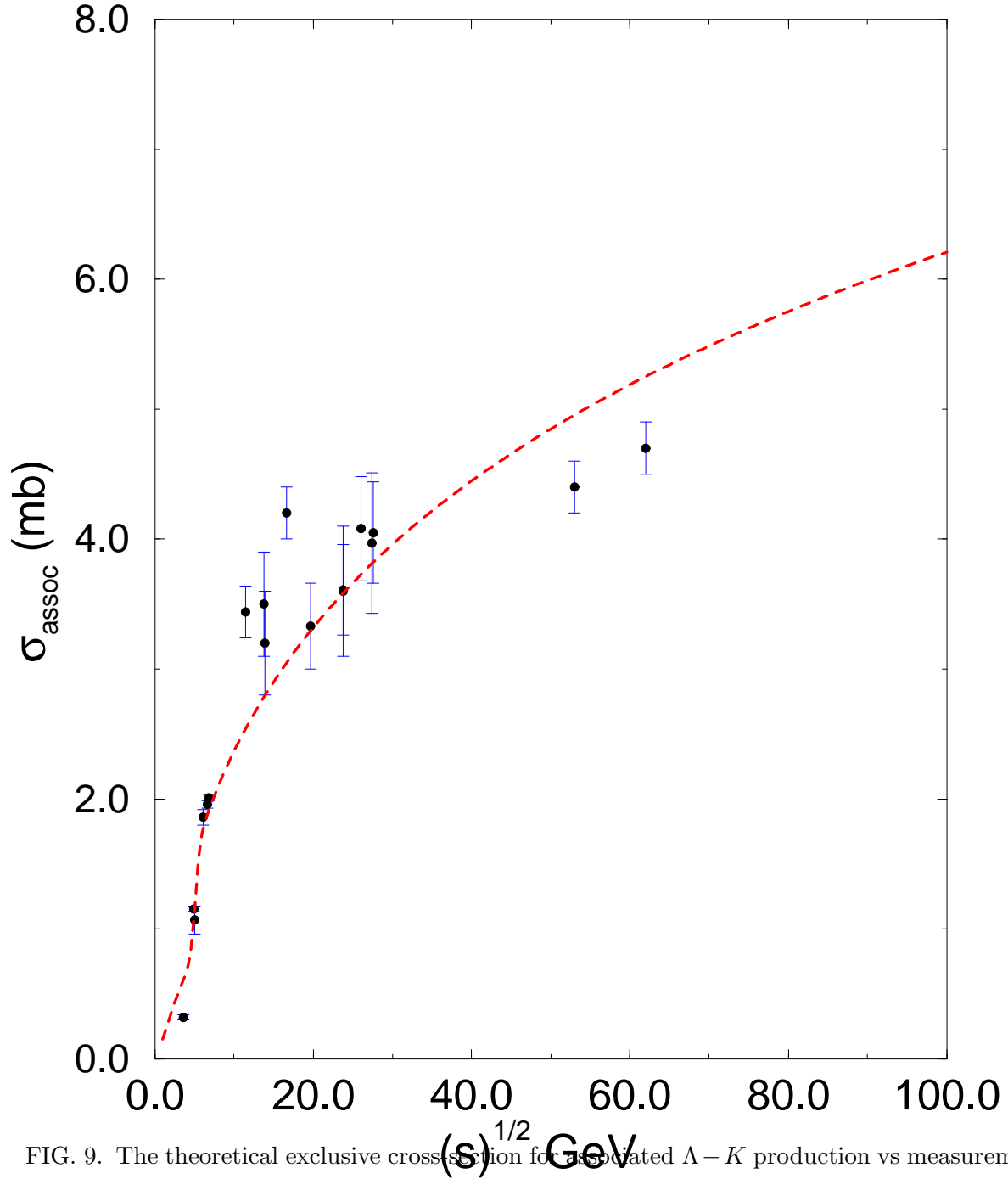


FIG. 9. The theoretical exclusive cross-section for associated $\Lambda - K$ production vs measurement. In the actual calculations we assumed the total production of all charged states of Σ hyperons equalled that into Λ .

String-Like Model for Hadron-Hadron Scattering

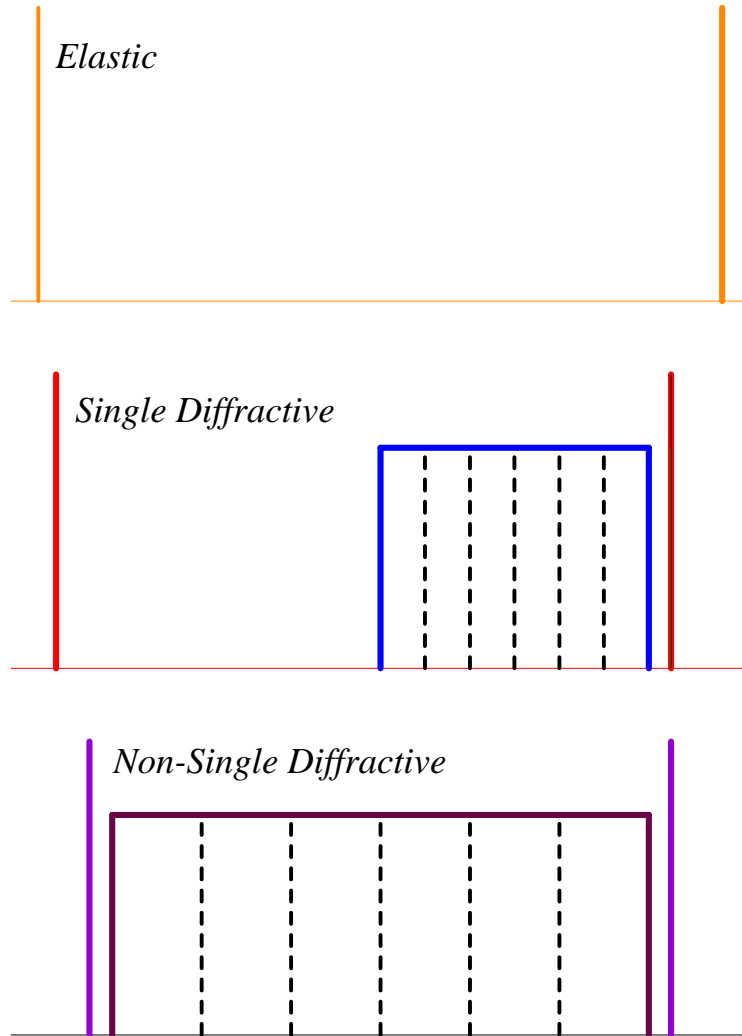


FIG. 10. Shown are graphic representations of the elements of the model for the elementary hadron-hadron collision: elastic, single diffractive (SD) and non-single diffractive (NSD). The meson groups introduced in both SD (with a rapidity gap) and NSD have a string-like character but are already sub-divided into generic resonances. It is customary to associate SD scattering with the three Pomeron coupling and NSD scattering with multi-Pomeron exchange.

$p+n \rightarrow \pi^-$ at $s^{1/2} = 19.4 \text{ GeV}$

Comparison with Eisenberg et al.

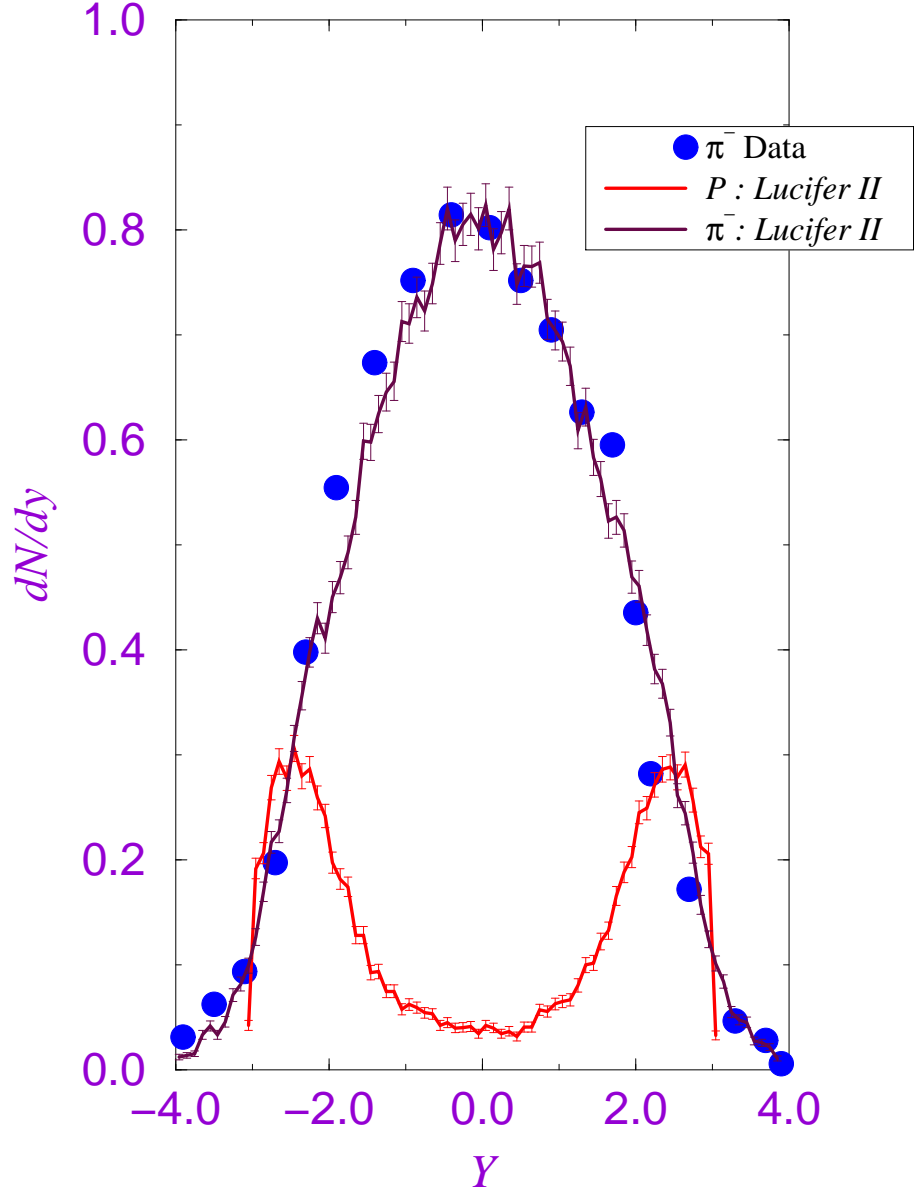


FIG. 11. The overall fit to the inclusive rapidity spectra for p and π^- from pn scattering at $\sqrt{s} = 19.4$, performed by Eisenberg et al. at FNAL

Initial Baryon Distribution

(after reinitialisation)

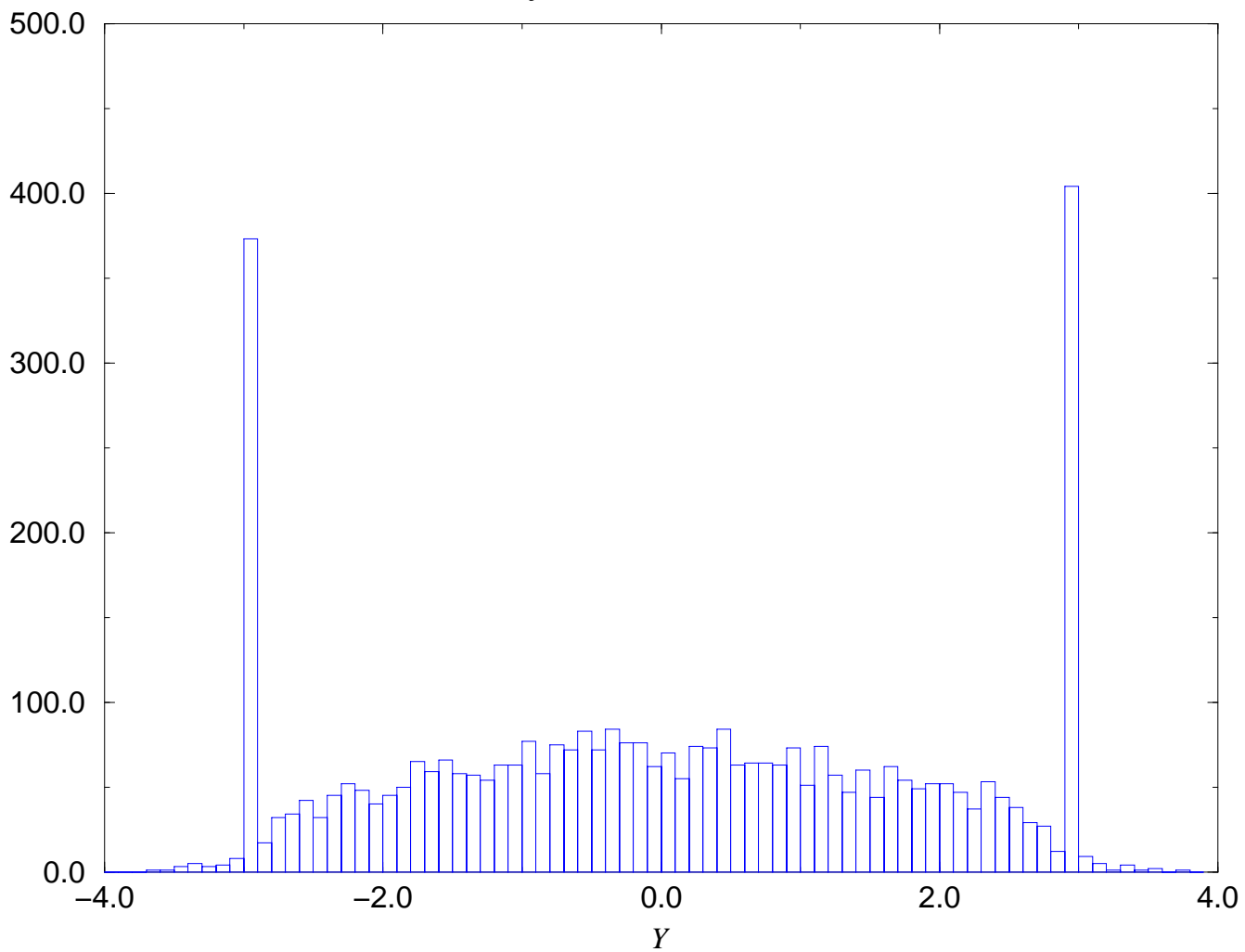


FIG. 12. Reinitialized rapidity spectrum for baryons in Pb+Pb, i. e. just before the start of the second stage, low energy cascade.

Initial Meson Distribution

(after reinitialisation)

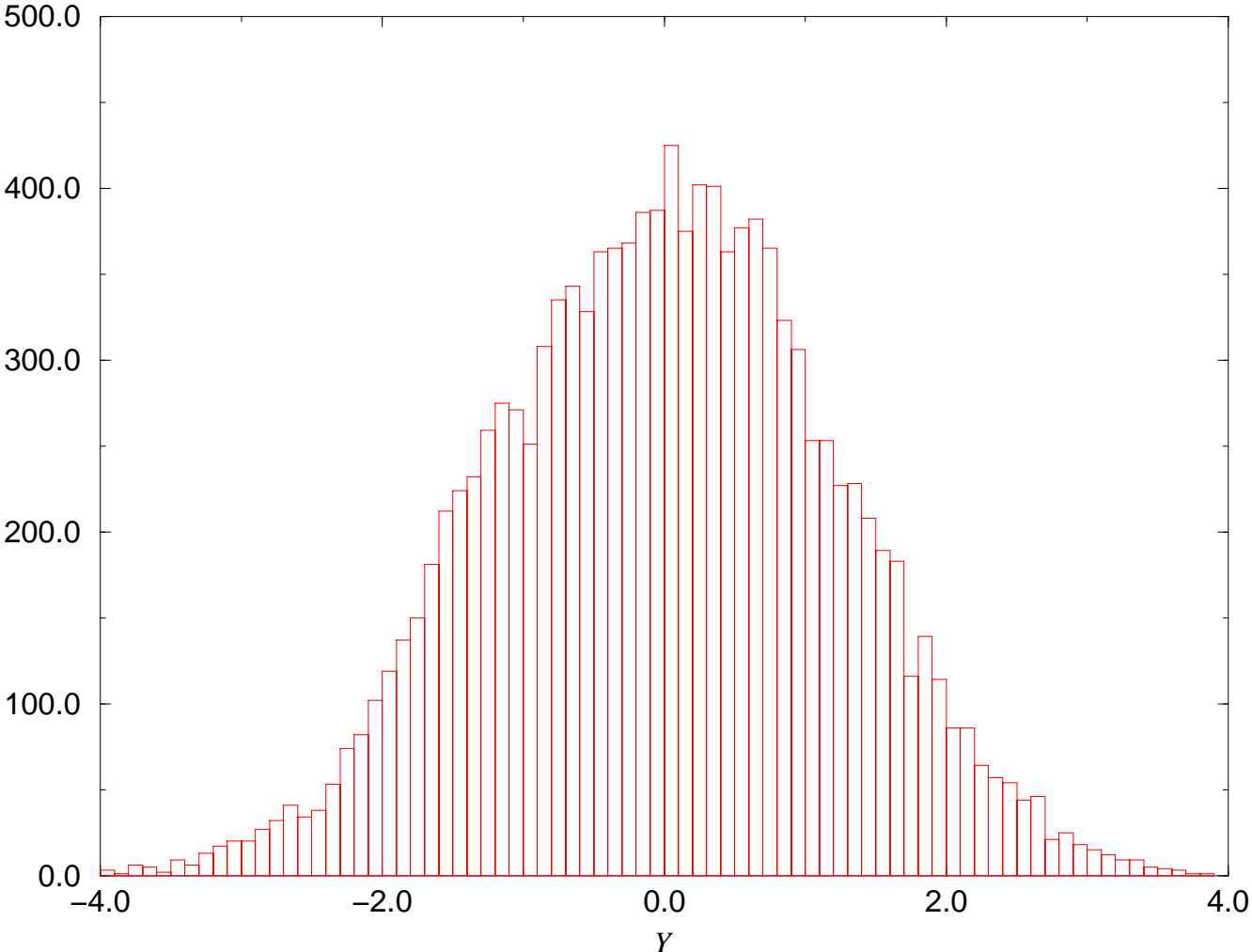


FIG. 13. Reinitialized rapidity spectrum for generic mesons in Pb+Pb, i. e. just before the start of the second stage, low energy cascade.

Initial Meson Interaction Positions

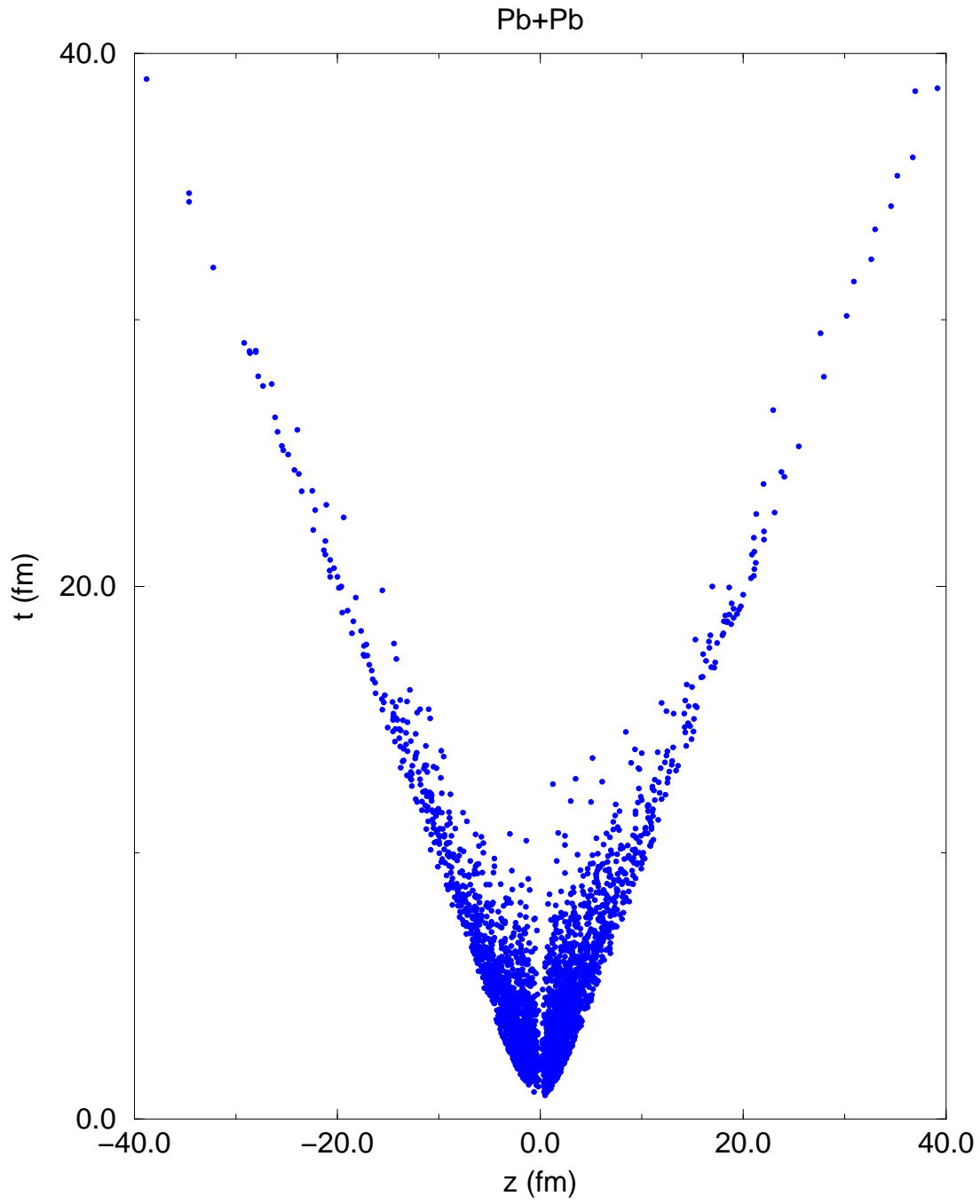


FIG. 14. Space-time distribution for generic mesons in Pb+Pb after the ~ 1 fm/c formation time. Mesons begin interacting in the second stage cascade only after reaching these positions.

Inclusive Distributions $S+S @ 200 \text{ GeV}/c$

NA35 Data vs Lucifer II

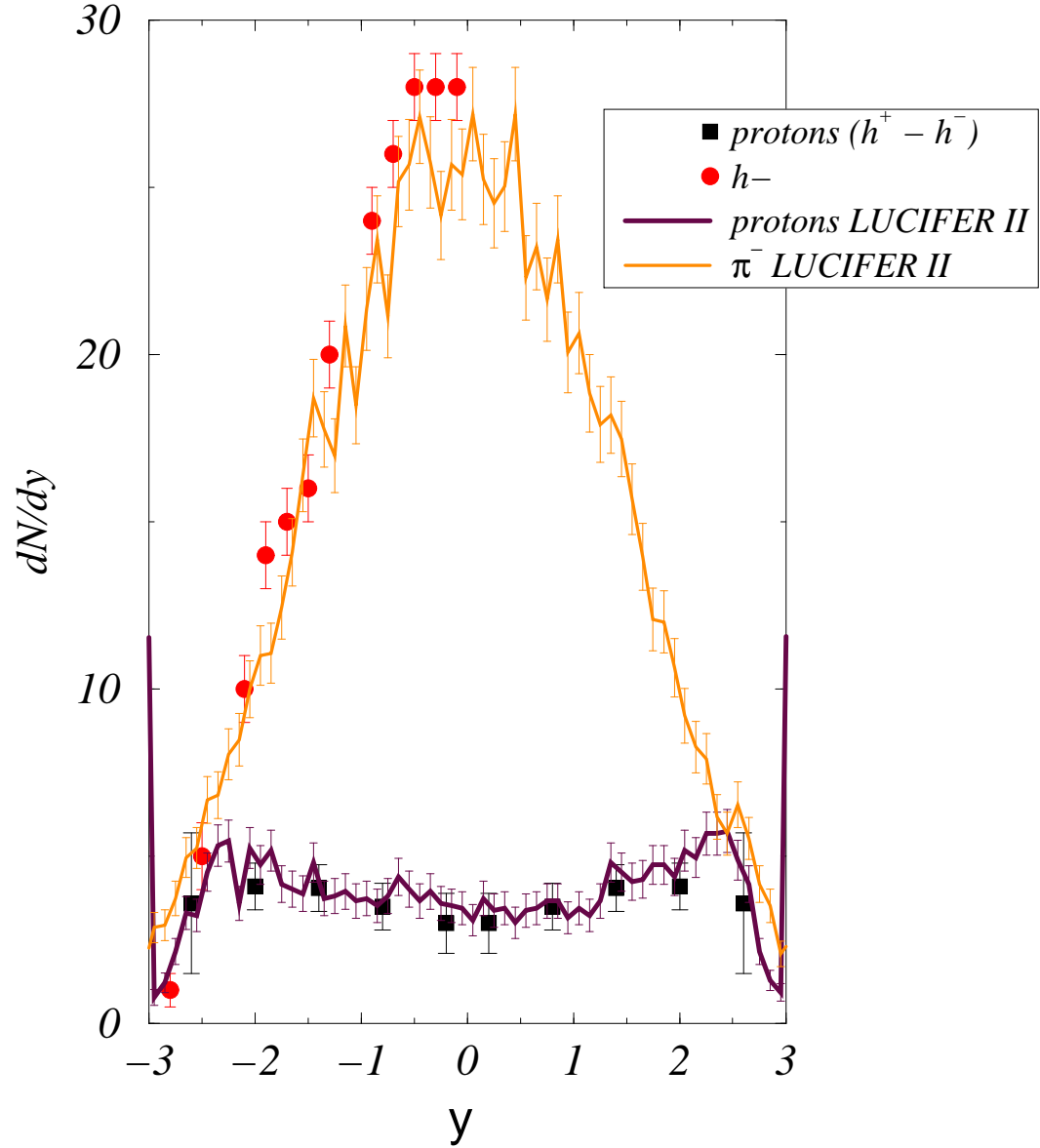


FIG. 15. The calculated $S+S$ rapidity spectra at $200 \text{ GeV}/c$ for π^- and protons compared to measurements by NA35. The latter are for total h^- and $h^+ - h^-$ respectively, but the experimental proton equivalent spectrum was corrected for the $K^+ - K^-$ contribution.

Inclusive Distributions: Pb+Pb @ 158 GeV/c
NA49 Data vs Lucifer II

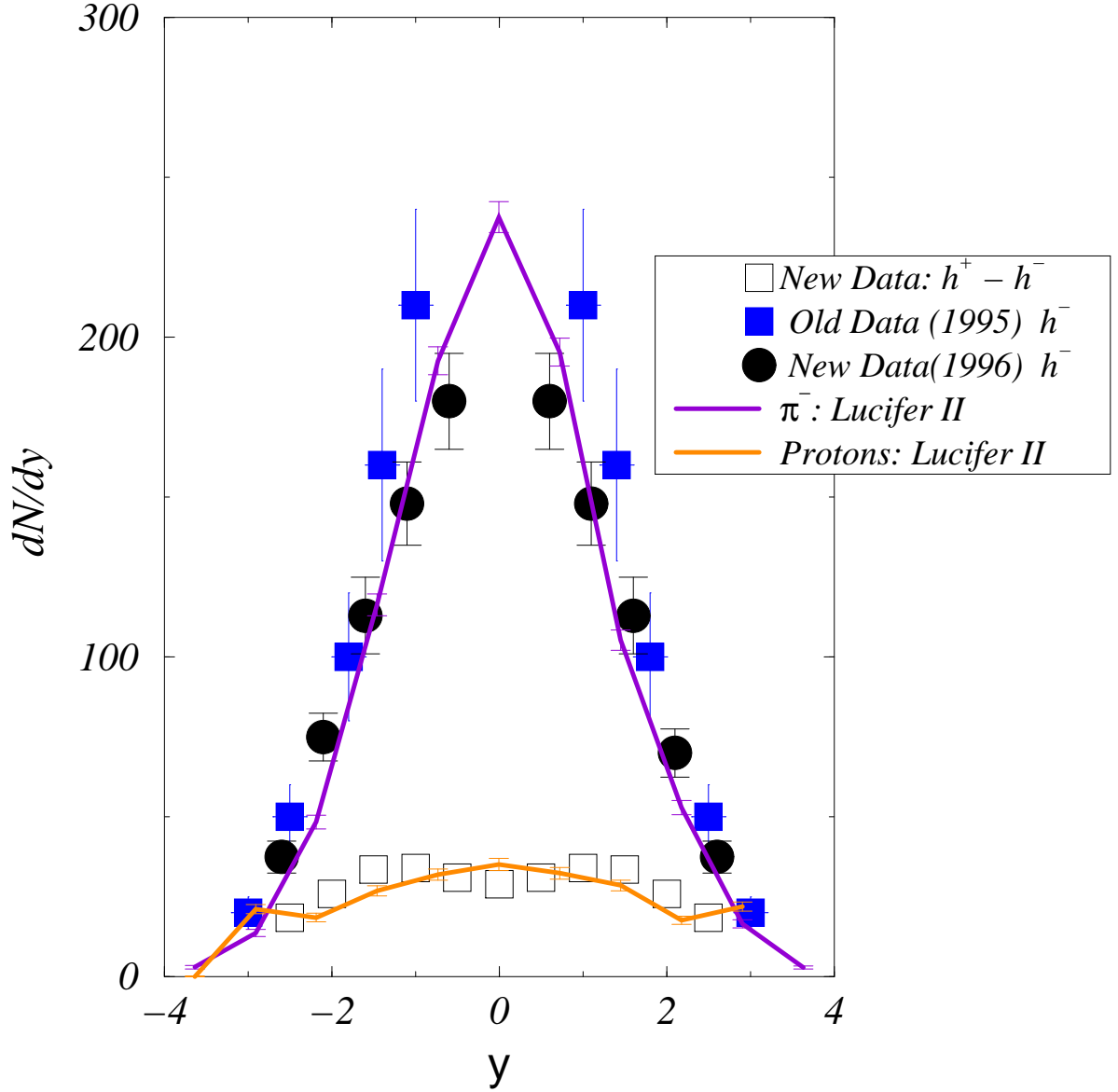


FIG. 16. The calculated Pb+Pb rapidity spectra at 158 GeV/c for π^- and protons compared to preliminary measurements by NA49. The latter are for total h^- and $h^+ - h^-$ respectively.

Proton Transverse Mass Distribution

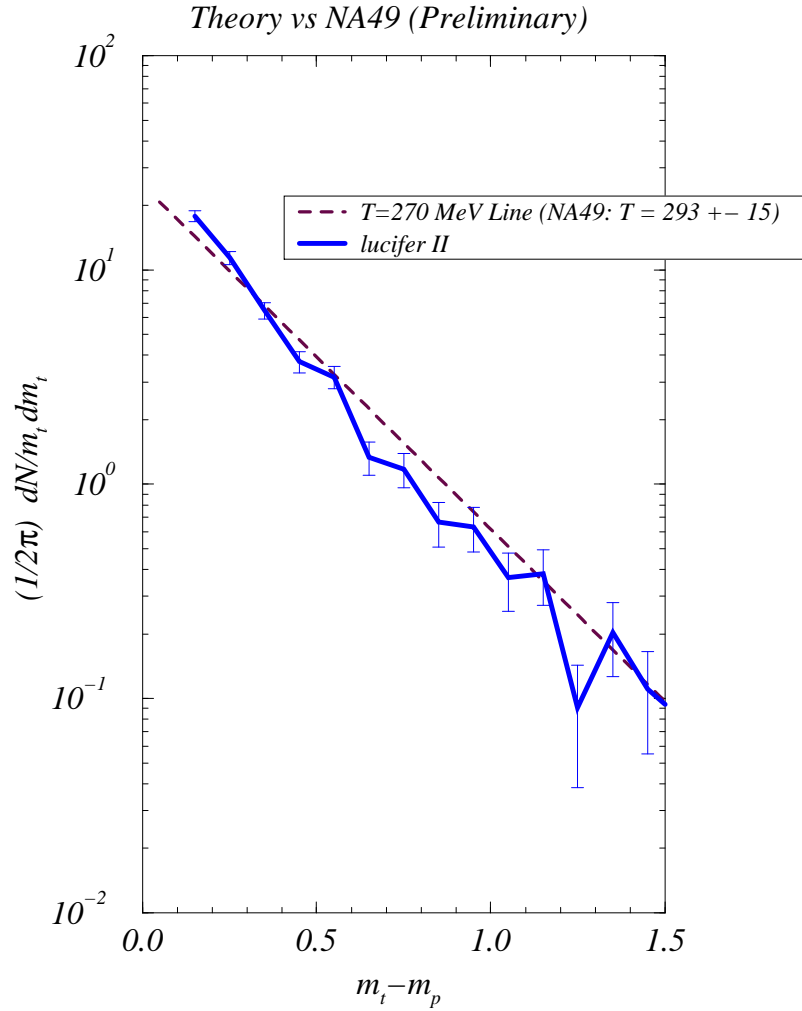


FIG. 17. A calculated transverse momentum spectrum for protons in Pb+Pb using a rapidity interval $-1.0 \leq y \leq +1.0$. Comparison is made to an exponential with inverse slope or ‘temperature’ T close to 270 MeV. The preliminary central NA49 value is $T=293 \pm 10$ MeV, for $-0.25 \leq y \leq 0.25$].

Lambda Transverse Mass Distribution

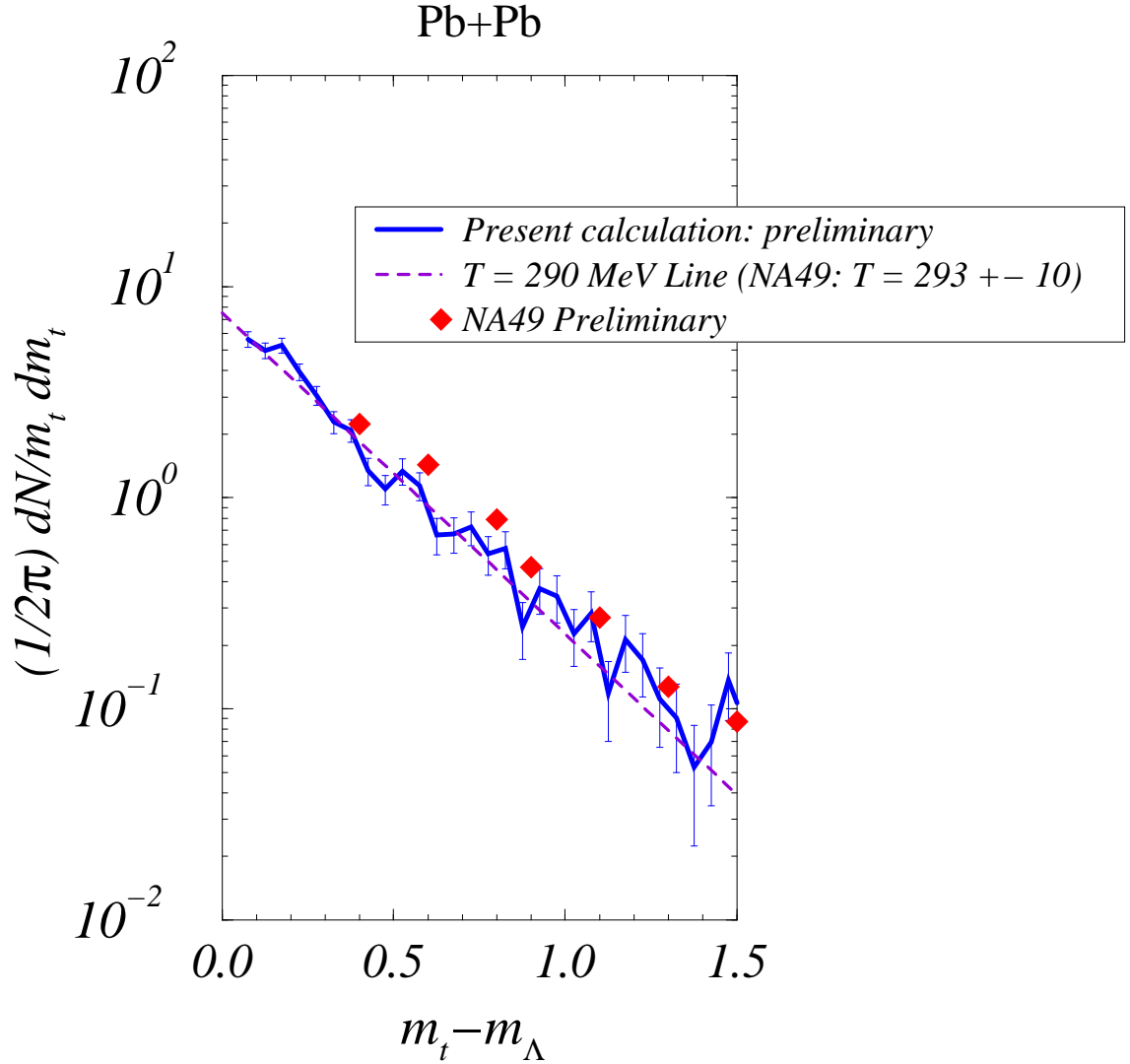


FIG. 18. A calculated transverse momentum spectrum for Λ in Pb+Pb using a rapidity interval $-1.0 \leq y \leq +1.0$. Comparison is made to preliminary NA49 data for central Pb+Pb.

Leading Particle Spectra

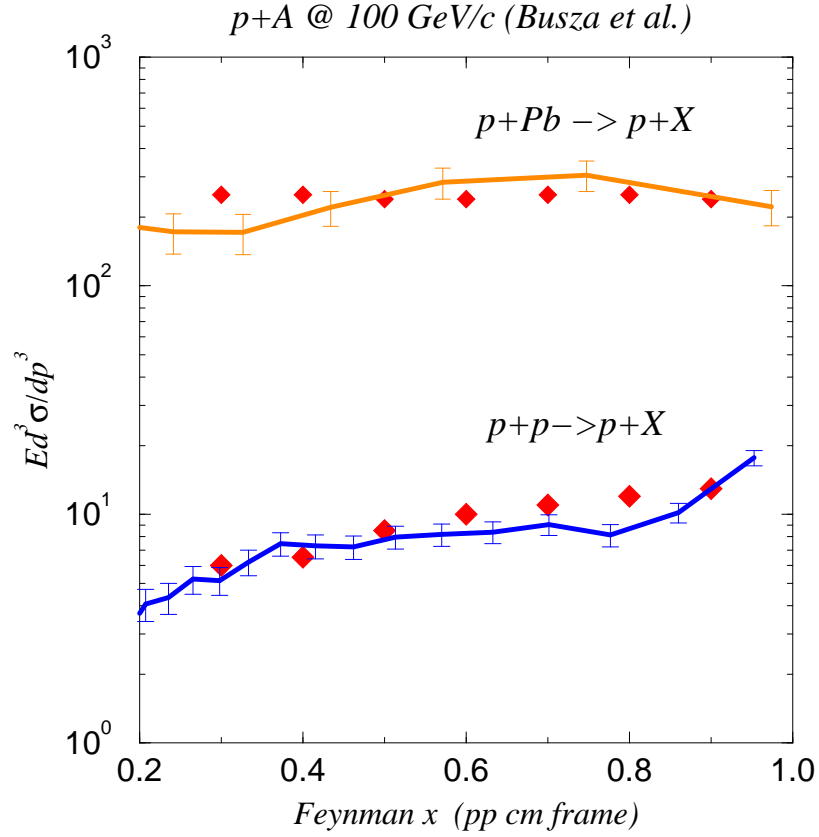


FIG. 19. Leading particle behaviour for inclusive proton production in pp and p+Pb. Simulations at 100 GeV/c are compared as a function of Feynman x to FNAL data from Busza et al. [17].

Drell–Yan A –Dependence (*Lucifer II*)

$p+A$ @ 800 GeV/c

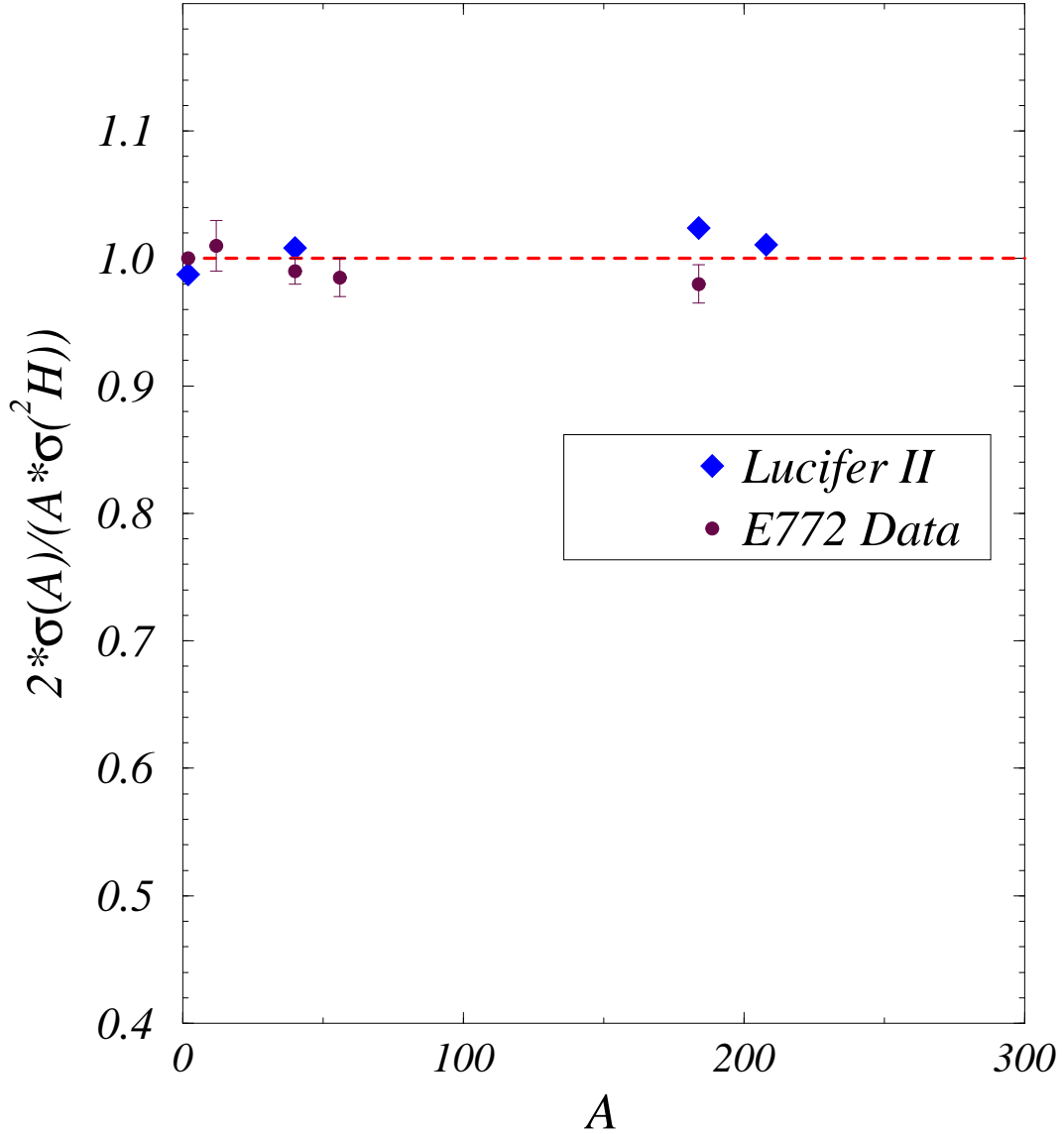


FIG. 20. Drell-Yan for pA . Similar to Figure 1 but with theoretical points added for a selection of nuclei. The only appreciable calculated production comes from the high energy phase and is essentially geometrical.